Copyright Warning & Restrictions

The copyright law of the United States (Title 17, United States Code) governs the making of photocopies or other reproductions of copyrighted material.

Under certain conditions specified in the law, libraries and archives are authorized to furnish a photocopy or other reproduction. One of these specified conditions is that the photocopy or reproduction is not to be "used for any purpose other than private study, scholarship, or research." If a, user makes a request for, or later uses, a photocopy or reproduction for purposes in excess of "fair use" that user may be liable for copyright infringement,

This institution reserves the right to refuse to accept a copying order if, in its judgment, fulfillment of the order would involve violation of copyright law.

Please Note: The author retains the copyright while the New Jersey Institute of Technology reserves the right to distribute this thesis or dissertation

Printing note: If you do not wish to print this page, then select "Pages from: first page # to: last page #" on the print dialog screen

ABSTRACT

DEVELOPMENT OF FLEXIBLE NICKEL-ZINC AND NICKEL-IRON BATTERIES

by
Xianyang Meng

The fabrication of flexible nickel-zinc batteries using a facile mixing of electroactive components for electrode preparation is presented. Polytetrafluoroethylene (PTFE) is found to be an effective binder by reducing concentration polarization, providing chemical/physical stability and enhancing flexibility. The zinc electrode containing PTFE maintains its original porous morphology even after hundreds of cycles while polymers such as PEO show morphology change. Each component, as well as the assembled flexible cells show desired flexibility and stability even under bending conditions.

The fabrication of flexible nickel-iron batteries using printable composite electrodes embedded with multiwalled carbon nanotubes (CNT) is also presented. All the metal oxides composites are one-step prepared by precipitation method of the metal oxides on the CNTs. After the deposition process, high loading ratio of conductive materials increases the efficiency of electroactive materials. Compared with $Ni(OH)_2$-CNT, β-NiOOH increases Fe_xO-CNT discharging voltage in flexible cells. All the components of flexible cells show good performance under bending conditions and even deeply bending conditions. Under low discharging currents, the Ni-Fe flexible battery shows a specific capacity of more than 300 mAh g^{-1} in 6 M KOH electrolyte saturated with LiOH, and 5% $Co(NO_3)_2$ in anode formulation. Furthermore, nickel-iron cell with Fe_xO-$CNT_{25.7}$ composite presents better results than using mixed Fe_2O_3 nickel-iron cell. Nickel-iron cells have better performance than nickel-zinc cells in rope batteries.

DEVELOPMENT OF FLEXIBLE NICKEL-ZINC AND NICKEL-IRON BATTERIES

by
Xianyang Meng

A Dissertation
Submitted to the Faculty of
New Jersey Institute of Technology
in Partial Fulfillment of the Requirements for the Degree of
Doctor of Philosophy in Chemistry

Department of Chemistry and Environmental Science

December 2018

APPROVAL PAGE

DEVELOPMENT OF FLEXIBLE NICKEL-ZINC AND NICKEL-IRON BATTERIES

Xianyang Meng

Dr. Somenath Mitra, Dissertation Advisor Distinguished Professor of Chemistry and Environmental Science, NJIT	Date
Dr. Tamara Gund, Committee Member Professor of Chemistry and Environmental Science, NJIT	Date
Dr. Robert B. Barat, Committee Member Professor of Chemical and Materials Engineering, NJIT	Date
Dr. Yuanwei Zhang, Committee Member Assistant Professor of Chemistry and Environmental Science, NJIT	Date
Dr. Mengyan Li, Committee Member Assistant Professor of Chemistry and Environmental Science, NJIT	Date

BIOGRAPHICAL SKETCH

Author: Xianyang Meng

Degree: Doctor of Philosophy

Date: December 2018

Undergraduate and Graduate Education:

- Doctor of Philosophy in Chemistry,
  New Jersey Institute of Technology, Newark, NJ, 2018

- Master of Science in Chemistry,
  New Jersey Institute of Technology, Newark, NJ, 2012

- Bachelor of Engineer in Pharmaceutical Engineering,
  Tianjin University of Technology, Tianjin, P. R. China, 2009

Major: Chemistry

Publications:

"Reducing Concentration Polarization and Enhancing the Performance of Flexible Nickel-Zinc Battery Using Polytetrafluoroethylene as Electrode Additive" Xianyang Meng, Zhiqian Wang, Giuseppe Di Benedetto, James L. Zunino, III, and Somenath Mitra. Chemistry Select, 2018.

"Synthesis of Carbon Nanotube-based Iron Oxides for the Development of Printable, Flexible Nickel-Iron Batteries" Xianyang Meng, Zhiqian Wang and Somenath Mitra. 2018. Under review.

"Synthesis of Carbon Nanotube Incorporated Metal Oxides for the Fabrication of Printable, Flexible Nickel-Zinc Batteries" Zhiqian Wang, Xianyang Meng, Kun Chen and Somenath Mitra. Advanced Material Interfaces, 2018.

"Development of High Capacity Periodate Battery with 3D-Printed Casing Accommodating Replaceable, Flexible Electrodes" Zhiqian Wang, Xianyang Meng, Kun Chen and Somenath Mitra. ACS Applied Materials and Interfaces, 2018.

"Development of Flexible Zinc-air Battery with Nanocomposite Electrodes and A Novel Separator" Zhiqian Wang, Xianyang Meng, Zheqiong Wu, Somnath Mitra. Journal of Energy Chemistry, 2016.

"Triple-stranded DNA Containing 8-oxo-7,8-dihydro-2'-deoxyguanosine: Implication in the Design of Selective Aptamer Sensors for 8-oxo-7,8-dihydroguanine" Qian Zhang, Yiqi Wang, Xianyang Meng, Rik Dhar and Haidong Huang. Analytical Chemistry, 2012.

"Synthesis of 3-Nitrobenzoic Acid" Zhang, Rui; Xiujie, Liu; Meng, Xianyang. The Conference Paper for 209 National Academic Conference on Organic Chemistry and Fine Intermediates, Tianjin, China, 2009.

爱人者人恒爱之。
Those who love people are always loved by other people.

Sincerely respect all the human being who dedicate to civilization constructively based on pure justice before, now and forever.

ACKNOWLEDGMENT

I would like to express my sincere appreciation to my dissertation advisor, Dr. Somenath Mitra for all his guidance and support. I would not have accomplished this project without your guidance and encouragement. I'm also grateful to all the committee members: Dr. Tamara Gund, Dr. Robert B. Barat, Dr. Yuanwei Zhang and Dr. Mengyan Li.

I want to thank Dr. Zhiqian Wang's for all his help for these years, and thanks to Dr. Megha Thakkar, Dr Jin Zhang, Dr. Kun Chen, Emine Karaman and Samar Azizighannad, who cooperated with me to generate sample data and to publish papers. I also sincerely thank to the other group members: Dr Sagar Roy, Worawit Intrchom, Madihah Humoud, Oindrila Gupta, Indrani Gupta and Mitun Chandra Bhoumick, for the formation of a good research environment with friendly encouragement.

I would like to thank my ancestors who gave me this good family environment and prominent relatives. Great thanks to my grandpa and people like him, who served as traditional medical doctors and surgeons—saved lives and cured ordinary people for almost free during their hard time and even war time. Their love for other people makes me want to dedicate something meaningful for other people in my life.

My thanks also to my parents, my wife, Xuan and all other families, friends and competitors who helped me directly and indirectly.

TABLE OF CONTENTS

TABLE OF CONTENTS
(Continued)

Chapter **Page**

LIST OF FIGURES

LIST OF FIGURES
(Continued)

CHAPTER 1

INTRODUCTION

1.1 Batteries

A battery is a device that converts its stored chemical energy directly into electric energy by electrochemical oxidation-reduction reactions. The rechargeable, also known as secondary, batteries can be recharged by a reversal chemical reaction process. A battery is composed of one or multiple cells, and a cell is the elementary electrochemical unit composed of electrodes (cathode/ positive electrode and anode/ negative electrode), separator (could be substituted by specific solid or gel electrolyte under circumstances), electrolytes, current collectors and container. During the discharge process, the anode gives up electrons to external circuit and is oxidized; the cathode accepts electrons via external circuit and is reduced. Either primary or rechargeable batteries are usually assembled and activated then ready for use. Reserve batteries is a kind of battery that at least one key component is separated from the rest of parts prior to activation for further use. Fuels cells require continuous feeding of active materials, which are not an integral part of the cell, into the cells when electrical energy is needed. [1]

For a cell with redox reaction shown in the below equations:

$$aA + bB \rightleftharpoons cC + dD \text{ (overall)}$$

$$aA + ne^- \rightleftharpoons cC \text{ (cathode)}$$

$$bB \rightleftharpoons ne^- + dD \text{ (anode)}$$

Generally, battery performance can be evaluated by capacity, energy, working voltage and cycle stability under various conditions.

The voltage of a battery, E, can be estimated by Nernst equation:

$$E = E_0 - \frac{RT}{nF} ln \frac{Ca^c Da^d}{Aa^a Ba^b}$$

where E_0 is the standard cell potential (electromotive force) based on standard electrode potentials, R is the gas constant, T is the temperature in Kelvin, F is Faraday constant, n is the electrons transferred in the reaction. Hence in a certain system, the changes in species activity, by means of increasing active material concentration or surface area, can slightly increase the output voltage of a battery cell. Besides, the higher chemical reaction rate leads to faster power delivery (high discharge rate).

Other factors affecting actual battery performance include, internal resistance, chemical deterioration (polarization, passivation, by-products, crystal structure change after cycles) of electrochemical materials and mode of charge/discharge. During storage and operation, self-discharge and memory effect from some battery systems will require specific methods like trickling charging and specific material preparation method to elongate the battery shelf life and cycling life, or they will tend to limit the performance and their application types. Costs also need to be considered a lot in real battery production for applications. Other than battery working performance, it is important to study further characteristics or effects on leakage, shock resistance, flammability involved with safety aspects on human and environment.

Zinc, iron, nickel, aluminum, magnesium and lithium are commonly used metals with relatively lower toxicity compared with lead, silver, cadmium and mercury. Zinc has been among the most popular anode material, especially in primary batteries, for its decent electrochemical behavior for battery reliability, proper solubility in aqueous solution, good availability for low cost. Iron has self-discharge properties and low discharge rate due to its low solubility in some alkaline battery environment. Nickel is a cost-effective metal for cathode and large surface area current

collector; Nonetheless, iron anode can usually provide the best cost-effective properties, extremely long battery life and safety for human and environment. Aluminum is also attractive for its electrochemical potential and abundance, but aluminum anode can be passivated easily under certain conditions. As a result, it requires more care than zinc and iron electrodes; Magnesium also has electropotential and is suitable for electrolyte with higher resistivity. Yet sometimes its negative electropotential can be a disadvantage on hydrogen generation during discharge and relatively poor storageability of a partially discharged cell. Lithium provides lightest weight for highest energy density and power density, though requires nonaqueous (some of them with certain toxicity) electrolytes in most cases and has safety issues after long-time cycling. Most common types of batteries include zinc-carbon batteries available as D, AA and AAA batteries; alkaline batteries in the form of AA, AAA, 9V batteries; lead acid batteries as car batteries; Ni-MH batteries also as rechargeable AA, AAA batteries; lithium ion batteries in cell phones, laptop computers and electric vehicles; zinc air and zinc silver batteries as button cells.

Many battery systems employ zinc as active anode. Typical systems are zinc-carbon battery, zinc-alkaline-manganese dioxides battery, zinc-air battery, zinc-silver oxide battery, nickel-zinc battery, zinc ion battery [2], zinc bromine flow battery [3] and zinc periodate battery [4].

Traditionally, the zinc-carbon is the most produced primary. Zinc-carbon cells use zinc anodes, MnO_2 cathodes and ammonium chloride and /or zinc chloride water-based electrolytes. Carbon black is mixed with the MnO_2 to improve conductivity and retain moisture. Zinc is oxidized and Mn(IV) is reduced to Mn(III). The chemical reactions are listed as follows depending on electrolytes:

$$Zn + 2MnO_2 + 2NH_4Cl \rightleftharpoons 2MnOOH + Zn(NH_3)_2Cl_2 \qquad \text{(Leclanché)}$$

$$Zn + 2MnO_2 + 2ZnCl_2 + 2H_2O \rightleftharpoons 2MnOOH + 2Zn(OH)Cl \qquad \text{(zinc chloride)}$$

This type of primary battery has been used and thrived over 150 years. The systems are reliable and used in low-power applications including flashlights, remote controls, toys and portable radios. In 1866, the first prototype of modern dry cell was a wet cell developed by Georges-Lionel Leclanché. In the 20th century the zinc carbon batteries gradually evolve, with improved MnO_2 and electrolytes. Especially, in the 1960s, zinc chloride cells were developed, improving heavy duty performance. The Leclanché zinc-carbon battery has advantages: low cost on cell, low cost per watt-hour, large variety of shapes, sizes, voltages, various formulations, wide distribution with availability and long tradition of reliability. At the same time, standard Leclanché battery also has many disadvantages: low energy density (65Wh/Kg in cylinder cell) and power density (100Wh/L), poor low-temperature performance, leakage problems under abusive conditions, low efficiency under high current drains, relatively low shelf life and steady voltage drop with discharge. Zinc chloride battery has higher energy density (85Wh/Kg) and power density (165Wh/L) than Leclanché zinc-carbon, wider working temperature range (-10 to 50 ºC), good lead resistance and high efficiency under heavy discharge loads. One of the disadvantages is mainly on requirement of excellent sealing system due to increased oxygen sensitivity.

In the category of secondary zinc batteries, Zn-alkaline-MnO_2 battery is a modified rechargeable version of primary zinc-MnO_2 battery. Zn-alkaline-MnO_2 battery uses zinc anodes, MnO_2 cathodes and alkaline electrolytes (normally KOH). It was marketed in the mid-1970s for 6V lanterns and portable TV sets. The half-reactions in alkaline environment are presented as follows:

$$Zn + 2OH^- \rightleftharpoons ZnO + H_2O + 2e^-$$

$$MnO_2 + H_2O + e^- \rightleftharpoons MnOOH + OH^-$$

Apparent advantages like low initial cost, produced in charged state (no activation required), maintenance free, no "memory effect" and nontoxic in Zn-alkaline-MnO_2 battery. For decades, the cycle life of a rechargeable Zn-alkaline-MnO_2 battery is shorter than other rechargeable batteries, and its capacity fades after cycles, especially with deep discharge. It also has higher internal resistance than Ni-Cd and Ni-MH batteries. In 2016, mild aqueous $ZnSO_4$-based electrolyte and α-MnO_2 nanofibres changed performance on zinc and manganese dioxides combination. The improvements on higher capacity (285 mAh /g), capacity retention (92% after 5000 cycles) and higher zinc stability were achieved. [5]

Iron is a good resource for active materials (cathodes and anodes) and current collectors in battery systems. Commonly used battery reactions are iron-air, iron-silver oxide, nickel-iron and lithium ion batteries.

Iron-air battery is a type of rechargeable metal-air battery, and the best sharing point of air related batteries is their cathode (air) need not to be sealed inside the batteries. In 1968, pioneers were working on Fe-air in NASA, and this type of battery reaction is still under further development on feasibility of automotive applications by European FP7 funded project, NECOBAUT.[6] The half-reactions in alkaline environment are presented as follows:

$$O_2 + 2Fe + 2H_2O \rightleftharpoons 2Fe(OH)_2$$

$$6Fe(OH)_2 + O_2 \rightleftharpoons Fe_3O_4 + 3H_2O$$

Fe-air battery has the advantages on decent energy density (50-75 Wh/kg), low cost, safety for human and environment. However, self-discharge, hydrogen evolution on charge and poor low temperature performance hindered this battery becoming a widely used one in applications.

When iron is used as cathode materials, the most widely used compounds are lithium iron phosphates in lithium ion batteries. During the charge-discharge cycles, other than the Li^+

intercalation, the iron valence is shifting between Fe^{3+} and Fe^{2+} redox couple.[7]

The structure of $LiFePO_4$ can provide high electronic conductivity, lithium ion and electron mobilities, and lithium iron phosphates are insoluble in the electrolyte with less flammability.[1] The main reaction of lithium ion battery with $LiFePO_4$ is describe below:

$$LiFePO_4 \rightleftharpoons FePO_4 + Li^+ + e^-$$

1.2 Flexible Power Sources and Their Applications

Flexible battery concept came out around 1960 [8-9], which contained the basic parts like ordinary batteries with flexible shape on all the parts, including anode, cathode, separator, electrolyte and current collector. **Figure 1.1** is a basic design of flexible battery. Meanwhile, the challenging point is to keep parts continuously contacting with each other, maintaining the overall reaction rate and reversibility during bending and cycling processes. As the development of all kinds of thin/flexible electronic applications: flexible screens, smart cards, intelligent labels, medical devices [10-13], flexible batteries have been more intensively studied in recent ten years [14-21]. Among these flexible batteries, lithium-ion batteries have high energy density [22] with certain limitations including safety issues [23-25]. The flexible power sources can also be combined with energy harvest devices like attaching to the other side of solar cell surface or windows and roofs from buildings High efficiency, low cost, more widely applied stable materials, formulations and proper production methods are desirable for flexible batteries. According to the reactions, the aqueous battery systems are cheaper on production and maintenance, more friendly to the environment than organic battery systems, even though they have less capacity and lower voltage.

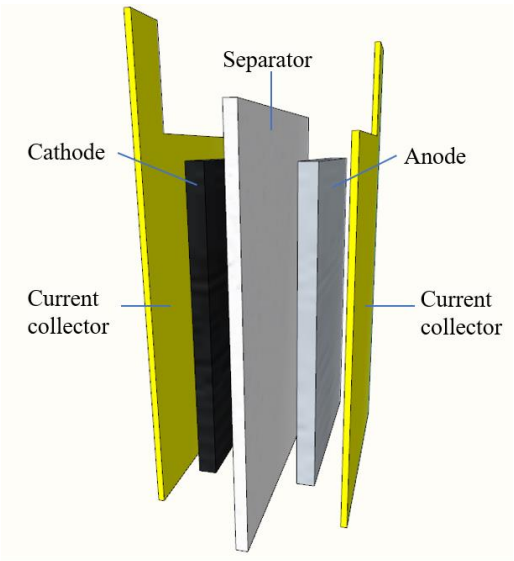

Figure 1.1 Basic design of a flexible battery.

1.3 Additives Related to Flexible Nickel, Zinc, Iron Electrodes

Additives are very important and widely used in both of rigid and flexible battery systems. The functions of additives vary according to their specific physical and chemical properties.

Binding additives are for the contact of each parts in side electrodes. In some researches, binders can be mixed with active electrode materials and to hold them together directly. Polyethylene oxide (PEO) and polytetrafluoroethylene (PTFE) are widely used binding additives, which are more stable than PVDF in alkaline-based battery systems [18, 26-28].

Conductive additives include two kinds: ionic and electric conductive additives. In some batteries, typical binding additives have the properties to react with each other, after absorbing active electrolyte, they served as gel electrolyte and separator at the same time [18, 29-30]. 1 g of copolymer made from polyvinyl alcohol (PVA) and polyacrylic acid (PAA) has the property to hold about 2.3g of 9M KOH electrolyte, and the ionic conductivity is properly maintained for the main reaction of flexible battery. As a result, the physical stability and ionic conductivity levels have been achieved properly by using PVP-PVA copolymer. It is also feasible to adjust the ionic

and electric conductivity together by creating internal wicking of electrodes. Cellulose [31], inorganic fibers and chopped newsprint are suitable to provide wicking channels. For example, as zinc dissolves in the electrolyte during discharge, the charging process may not restore the original high surface area of zinc metal, which leads to low active material utilization; then cellulose, like methyl cellulose can solve this problem.

More conductive additives are for electrical conductivity: carbon materials, conductive polymers, conductive metal and metal oxides are broadly employed in battery models. The prominent conductivity and stability with low cost properties keep them useful and developing. The layer structural graphite and grape shape carbon black provided decent conductivity and surface area for electrode active materials. Due to high electrical conductivity and large surface area, carbon nanotubes (CNTs) and graphene materials have attracted much attention as effective conductive additives in aqueous cells and metal ion batteries. [32] Additionally, the great mechanical properties, including high strength and flexibility, make CNTs very promising component for thin layer and flexible electrodes. [14, 16, 18, 33] With CNTs and graphene combined together, researchers also invented ultrafast rechargeable batteries. [34-35] Electrically conductive polymers are another subtype additive. Conductive polymers are amorphous (more elastic flexibility) with only a little diffraction. Then carbon materials like CNTs are more rigid, which has nanometer level scaffold functions. For instance, poly(3,4-ethylenedioxythiophene) polystyrene sulfonate (PEDOT: PSS) is a conductive polymer mixture of two ionomers. In PSS, part of the sulfonyl groups is deprotonated and negatively charged. PEDOT is a conjugated polymer and carrying positive charges. PEOT: PSS in aqueous zinc-carbon battery[33] and lithium ion battery[36], Polypyrrole (PPy) and Polyaniline (PANI) mixed with $LiFePO_4$[37] showed excellent performance. However, conductive polymers have disadvantages on chemical and physical stabilities under high temperature and oxidizing

conditions. Metal and metal oxides also worked well as conductive additives. Micro size three-dimensional nickel foam is a popular current collector to improve conductivity and utilization of active materials. In cathodes with oxidizers, nickel foam and carbon materials also could be oxidized on their surfaces, but nickel foam would not introduce carbonates that slowly destroy the alkalinity of electrolytes. Zinc oxide has low conductivity among metal oxides. ZnO and $Zn(OH)_2$ surface passivation occurs when the concentration of discharge products reaches a solubility limit. Addition of bismuth and lead solved this kind of problem. [38] The electrical conductivity of titanium dioxide is top among metal oxides, making this kind of high conductive metal oxides and ceramics decent additives and frames for electrodes [39-40].

To improve the performance of batteries on capacity, charge-discharge rate, cycle lives and voltages. Additives were used as side reaction and shape change inhibitors. Corrosion is one of the side reactions need to be avoided during storage. Zinc corrosion in alkaline solution is cathodic controlled, so the rate of the cathodic hydrogen evolution limits the zinc corrosion rate. Organic additives, typically polyethylene glycol like PEG400, was especially effective to inhibit corrosion [41]. In zinc anode batteries, calcium oxide introduced calcium zincate, which has lowered solubility than zinc hydroxides. Therefore, less zinc shape change and the longer cycle lives accomplished with addition of calcium. [42-43]

Functional groups like hydrophilic carboxylic groups can be generated on the surface of CNTs, changing many characteristics including the dispersibility in water, conductivity and redox properties. Microwave treatment of CNTs is known to cause in-situ super heating resulting in fast reaction rates and high degree of functionalization [44-45]. Microwave method were also used to purify CNTs by removal of functional groups and metals. [46] The purification processes of CNTs

were commonly achieved in the microwave accelerated reaction system by dispersing pre-weighed CNTs into dilute strong acids like HNO_3 and H_2SO_4.

Consequently, researches have been focused on flexible Ni-Zn and Ni-Fe batteries under flat and bending conditions. The studies contain production processes, including design of the cells, active material preparation, additives, current collectors, separators and formulations.

CHAPTER 2

REDUCING CONCENTRATION POLARIZATION AND ENHANCING THE PERFORMANCE OF FLEXIBLE NICKEL ZINC BATTERY USING POLYTETRAFLUORETHYLENE AS ELECTRODE ADDITIVE

The objective of this research is to develop flexible electrodes by facile mixing of ingredients and study different binders. Of particular interest to this research is to investigate the potential use of PTFE as a binding additive for Ni-Zn batteries

2.1 Nickel-zinc Batteries

Compared to other nickel-based batteries, Ni-Zn cells can provide a higher discharge voltage and hence higher output power than Ni-MH batteries. The stable discharge voltage of Ni-Zn battery is around 1.5V, which is higher than 1.1V from Ni-MH. Ni-Zn battery has higher energy density than batteries like lead-acid and Ni-Cd. The energy density and power density level is lower than lithium ion battery, but it is still very comapreable with lithium ion battery by other advantages. Lower cost is caused by the abundance of active materials (zinc and nickel compounds), aqueous electrolyte and relatively easy production process. Water based, akaline, non flamable electrolyte also provide better safty level than electrolytes in lithium ion batteries. Nickel and zinc can be recycled from this aqueous battery, and they do not have tthat much burden like cadmium, lead and mecury [47]. Decent working voltage and capacity can be achineved from -10 to 60℃. [1]

2.2 Challenges of Making Flexible Nickel-zinc Batteries

Fabricated into various shapes and sizes, conformal and flexible batteries have the potential to power up the next-generation flexible electronics [11, 48-51], medical, energy harvesting and wearable devices [52-55]. Traditional batteries such as zinc-carbon [20, 56-57], alkaline [18, 58], zinc-air [16, 59] and lithium-ion cells [17, 21, 60-61] can be converted into flexible designs by introducing novel material and formulations. Lithium-ion batteries have high energy density [22] but face certain limitations including safety issues especially when fabricated on polymer films [23-25]. At the same time rechargeable alkaline cells [62-65] show a drop in capacity after a few cycles. Secondary Nickel-Zinc batteries are safe, use aqueous electrolytes and both nickel and zinc are available in abundance. Compared to other nickel-based batteries, Ni-Zn cells can provide a higher discharge voltage and hence higher output power than Ni-MH batteries. There are a few reports on flexible Ni-Zn cells [50-51, 66-69], which are mostly binder-free. However, the fabrication processes for these electrodes are complicated where nanomaterials are deposited or grown on conductive substrates such as carbon [51, 70-71] and metal [50] to achieve high surface area and conductivity. In the area of fabrication of printable flexible batteries, a key ingredient is the polymer binder that provides the desired flexibility, inhibits side reactions, and enhances conductivity. The binder should not dissolve in the electrolyte and they should not react with electroactive ingredients.

2.3 Flexible Nickel-zinc Cell Fabrication

The active nickel pretreatment was carried out by mixing 9.27g Nickel (II) hydroxide (Strem Chemicals), 28.0 g KOH (Sigma, pellets, ≥ 85%) and 300 mL Clorox (9% chlorine). This process converted Ni(OH)2 to NiOOH. The solution was stirred and heated at 60 °C until no visible liquid was left. The solid was washed with 1 L 5% KOH solution, filtered and dried under vacuum at room temperature. Then dried solids were ground into a fine powder for future use. The cathode formulation comprised of nickel, polyethylene oxide (PEO, Sigma Aldrich, MW~400,000) binder and conductive additives such as multiwalled carbon nanotubes (MWCNTs, purity 95%, diameter 20-30 nm, length 10-30 μm, Cheap Tubes Inc. Brattleboro, VT, USA). After mixing the chemicals in DI water, the formed paste was sonicated for at least 30 minutes using an ultrasonic homogenizer (Omni Sonic Ruptor 250) and then stirred for 2 hours to form a homogenous slurry. A typical dry cathode contained 80% prepared NiOOH, 10% PEO and 10% MWCNTs. The chemicals were mixed in DI water and stirred for 2 hours before use.

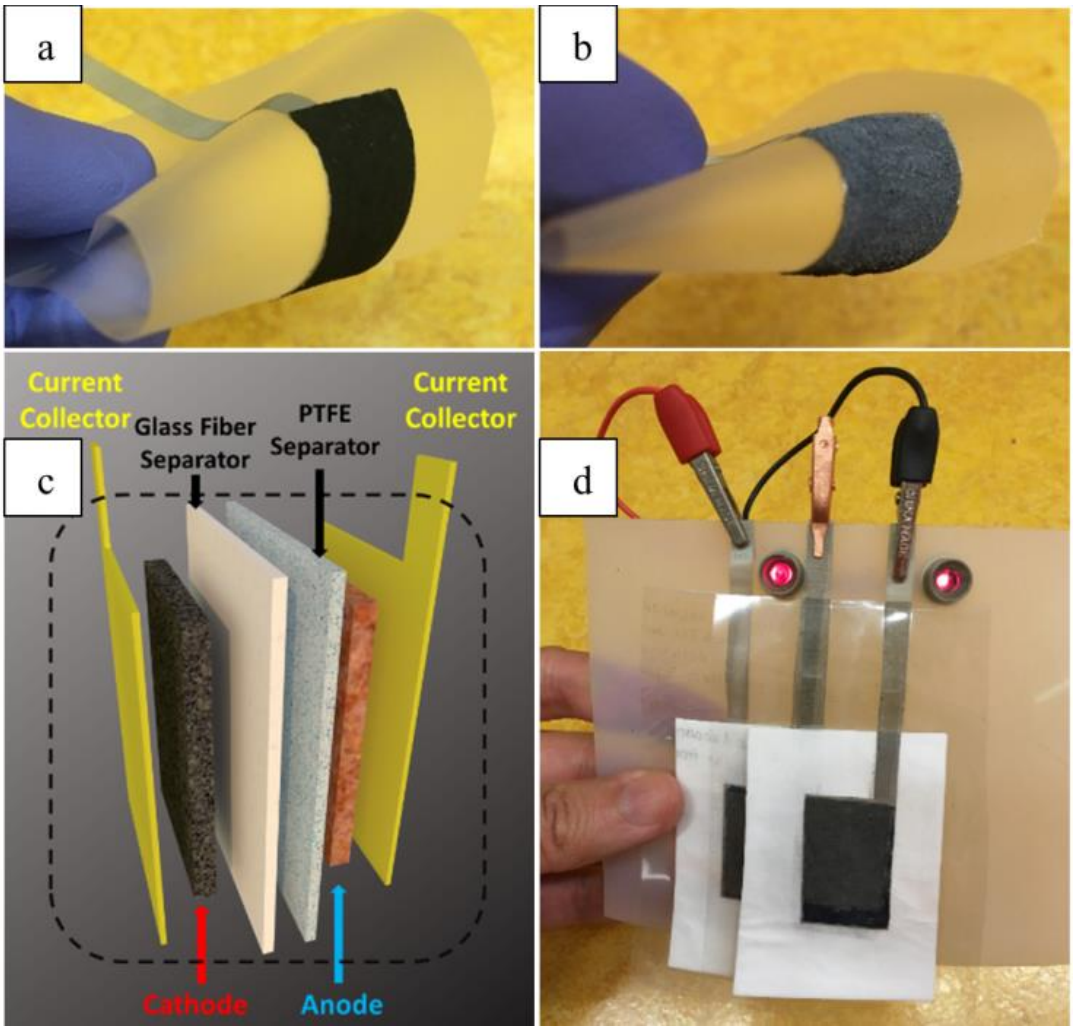

Figure 2.1 (a) flexible cathode; (b) flexible anode; (c) structure of a flexible secondary Ni-Zn battery; (d) flexible cells powering LED lights.

Depending upon the formulations, the anode comprised of battery grade zinc powder (Umicore, BIA 100 200 65 d140, ≤ 425 μm), polymer binder, zinc oxide (Sigma Aldrich, ≥ 99%), methyl cellulose (Sigma Aldrich, Mn~40,000), bismuth (III) oxide (Sigma Aldrich, 90-210 nm particle size, ≥ 99.8%) corrosion inhibitors [38], and multiwalled carbon nanotubes (MWCNTs). The powders were mixed in the DI water and then stirred to form a homogeneous paste. The anode slurry was stirred for 1 hour to avoid extra zinc

oxide formation. A typical dry anode contained 4% MWCNT, 3% PTFE and 3% Bismuth (III) oxide. The mass ratio of zinc, zinc oxide, conductive additives were varied. Swagelok-type cells used to optimize electrode formulation. The electrolyte was the mixture of 8.5 M KOH and 0.5M NaB_4O_7 with saturated ZnO [67]. For cyclic voltammetry electrodes, micron-sized chemical grade zinc (Sigma Aldrich, ≤10 μm, ≥ 98%) was also used.

Flexible electrodes were prepared by spreading the electrode slurry onto the current collectors. The standard flexible electrode was 3 x 2 cm. Copper tapes (EMI Copper Foil Shielding Tape 1181, 6.35mm, 3M™) were attached to the current collectors to serve as electrode tabs. After the slurry was pasted on the current collectors, the anodes and cathodes were dried at room temperature for 2 and 4 hours, respectively; and their corresponding weights were 0.03 g and 0.05 g. In a flexible cell, all layers were sandwiched and thermal sealed.

Figure 2.1 showed the structure of the battery, as well as photographs of flexible electrodes after drying. In all the cells tested, zinc was in stoichiometric excess to maintain the required anode conductivity. Silver ink, copper tape, copper mesh, stainless steel 304 mesh (wire diameters 0.1651 mm and 0.03556 mm) and graphene ink (Tanfeng Technologies. Jiangsu. China) were tested as current collectors. Current collectors made from conductive inks were dried for 12 hours in fume hood at room temperature to avoid fast drying induced cracking. Silver current collectors were prepared by brushing silver ink (Circuit Writer, CAIG Laboratories. Inc.) with acetone (mass ratio 1:1) onto the adhesive side of polyethylene terephthalate (PET) film coated with ethylene vinyl acetate copolymer

(EVA) resin (CRC52005, 3 mil, Fellowes). Glass Fiber (Whatman, Grade GF/A 1.6μm), hydrophilic PTFE (Hangzhou ANOW Microfiltration, pore size 5μm) separators and their combinations were tested in this flexible battery model individually.

2.4 Materials Characterization for Flexible Nickel-zinc Cells

Figure 2.1a and b are photographs of typical thin-film electrodes showing flexibility. Structure of the battery is shown in Figure 2.1c. The flexible separator combination comprised of a glass microfiber on the cathode side and hydrophilic PTFE on the anode side. The flexible separator was placed between the electrodes, and the assembled cells are shown powering LED lights in Figure 2.1d. **Figure 2.2** shows the SEM images of NiOOH and the prepared electrodes. The NiOOH particles used for cathode were in micron range. Carbon nanotubes can be seen distributed in the cathode leading to the formation of conductive networks.

2.5 Optimization of Flexible Nickel-zinc Cells

2.5.1 Nickel Oxyhydroxides and Multi-walled Carbon Nanotubes

Oxidation state of the Ni was critical to the performance of the Ni-Zn cells. Commercial green $Ni(OH)_2$ was pre-oxidized to black NiOOH and the resulting material was used as the active cathode material. The major benefit of pre-oxidation was that the NiOOH was in a charged state and the assembled battery was ready for use. Figure 2.2 shows the SEM images of NiOOH and the prepared electrodes. The NiOOH particles used for cathode were

in micron range. Carbon nanotubes can be seen distributed in the cathode leading to the formation of conductive networks. XRD results of the oxidized Ni is shown in **Figure 2.3**. The main peaks were at 19.01° (001), 33.09° (010), 38.56° (011), 52.10° (012) and66.02° (110) (ICSD 98-016-9978, ICDD 00-006-0141) indicated the existing of β-structured $Ni(OH)_2$ and NiOOH [72-73]. Like conventional Ni(OH)2 batteries, overcharging would lead to the transformation of β-NiOOH to the larger γ-NiOOH [25] particles, which is known to cause significant electrode size/shape change. This could lead to electrode cracking and disintegration, compromising the both performance and flexibility. In a flexible cell with limited space, even partial formation of γ-NiOOH could penetrate the separator and destroy the cell.

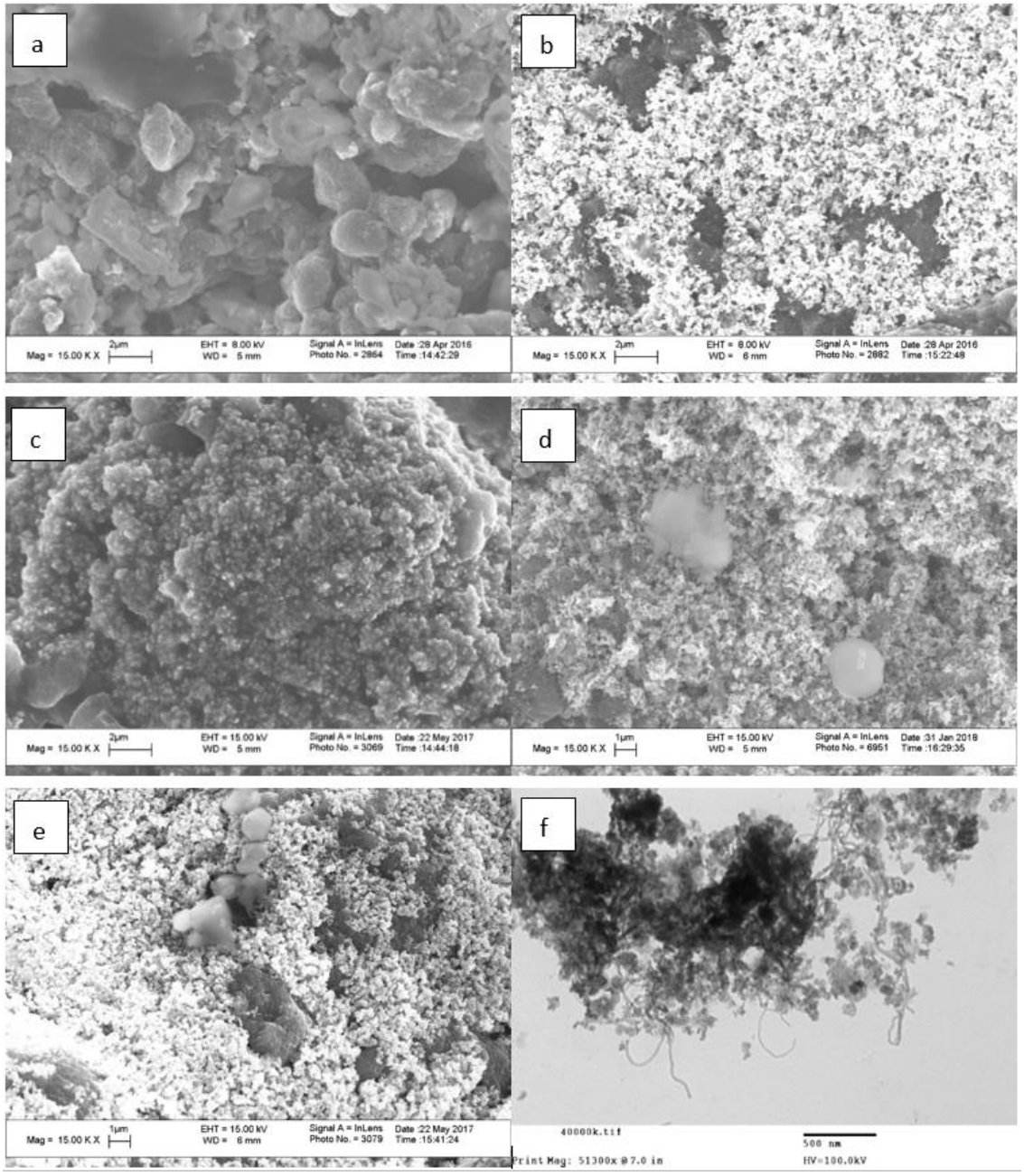

Figure 2.2 SEM images of (a) cathode materials; (b) anode with PEO before charge-discharge cycles; (c) anode with PEO after charge-discharge cycles; (d) anode with PTFE before cycles; (e) anode with PTFE after cycles. (f) TEM image of cathode with MWCNTs.

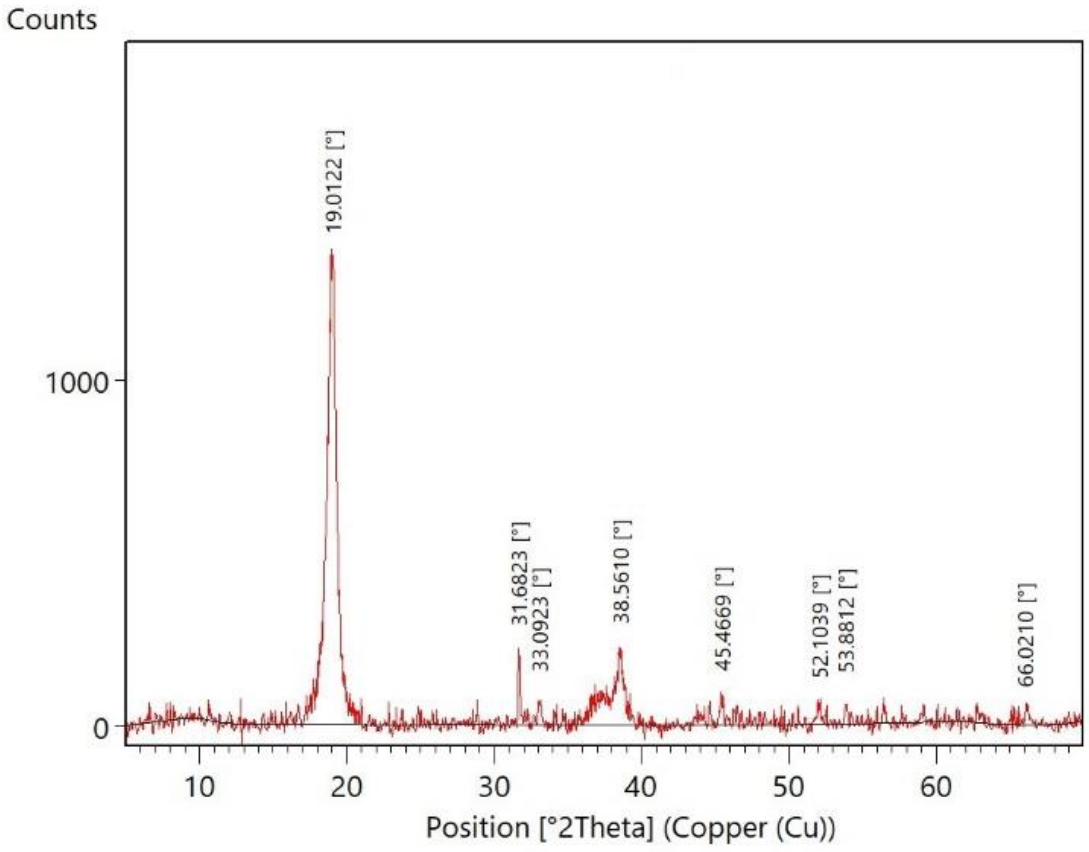

Figure 2.3 XRD of pre-treated NiOOH.

Due to the low conductivity of metal oxides and hydroxides, conductive additives are required, and as mentioned before MWCNTs were quite effective for electrode applications [74-78]. It was found that high amount MWCNTs made the battery unstable [18]. Furthermore, higher amount of non-reactive materials would occupy the valuable space in the electrochemical cell and 4% MWCNTs in cathode showed the best performance (Figure 2.4).

Stainless steel 304 mesh was found to be the best current collector and was better than silver paste, which tended to be corroded by high valence nickel.

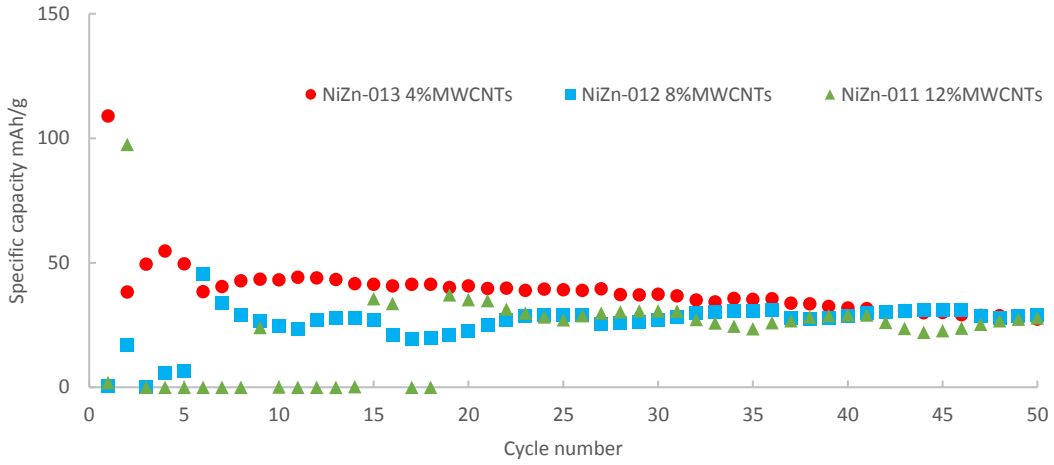

Figure 2.4 Cathode conductive additive optimization in Swagelok cells.

2.5.2 Effects of Polymer Additives and Separators

Different polymers were tested as anode binding additives. PVP and PAA were found to be soluble in KOH, PVDF decomposed in KOH while PEO and PTFE showed adequate stability. PEO and PTFE were both electrically non-conductive; however, PEO is known to be ionic conductive in KOH [79-80]. Although PEO is water soluble, it is insoluble in strong alkaline media such as concentrated KOH solution. PTFE is highly hydrophobic, chemically stable [81-83] and has been used in rigid batteries including Ni-Zn [66, 78], Li-O2 [84] and MnO2-Zn [85]. In this study, PEO and PTFE were tested and compared as binding additives. After several cycles, the cells with PEO failed while those with PTFE lasted much longer (**Figure 2.5**).

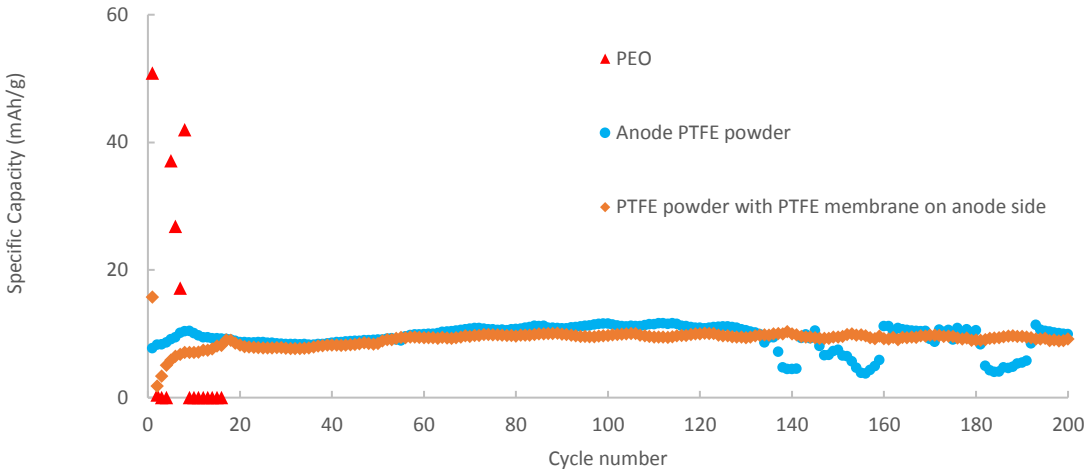

Figure 2.5 Discharge capacities comparison in different flexible cells: 1. PEO only 2. PTFE binder in anode. 3. PTFE binder along with PTFE separator on anode side.

The degradation of anode materials with cycling is an important issue for all rechargeable batteries. Another purpose of polymer additives, especially in zinc secondary anodes, was to provide channels for electrolyte and avoid the formation of an inert layer on anode surface. Methylcellulose has been added into zinc anode as a gelling agent to prevent the alteration of anode morphology [63, 65]. In this study, the anodes with PEO showed significant changes in morphology after a few charge-discharge cycles (Figure 2.2b and c) with reduced pores and channels for electrolyte. However, the electrodes with PTFE remained porous (Figure 2.2d and e) and did not show as many alterations. No significant change in the color, hardness or shape change was observed after hundreds of cycles with the PTFE binder. At the micrometer scale, the zinc anode surface with PEO was rough after cycling (**Figure 2.9a**) while the anode surface with PTFE remained flat after many cycles (**Figure 2.9b**), as observed through optical coherence tomography (OCT) [86]. Furthermore,

PTFE also increased the flexibility of the electrodes. Cells with a thin layer hydrophilic PTFE membrane separator on the anode showed more stable cycling than the ones without (Figure 2.5).

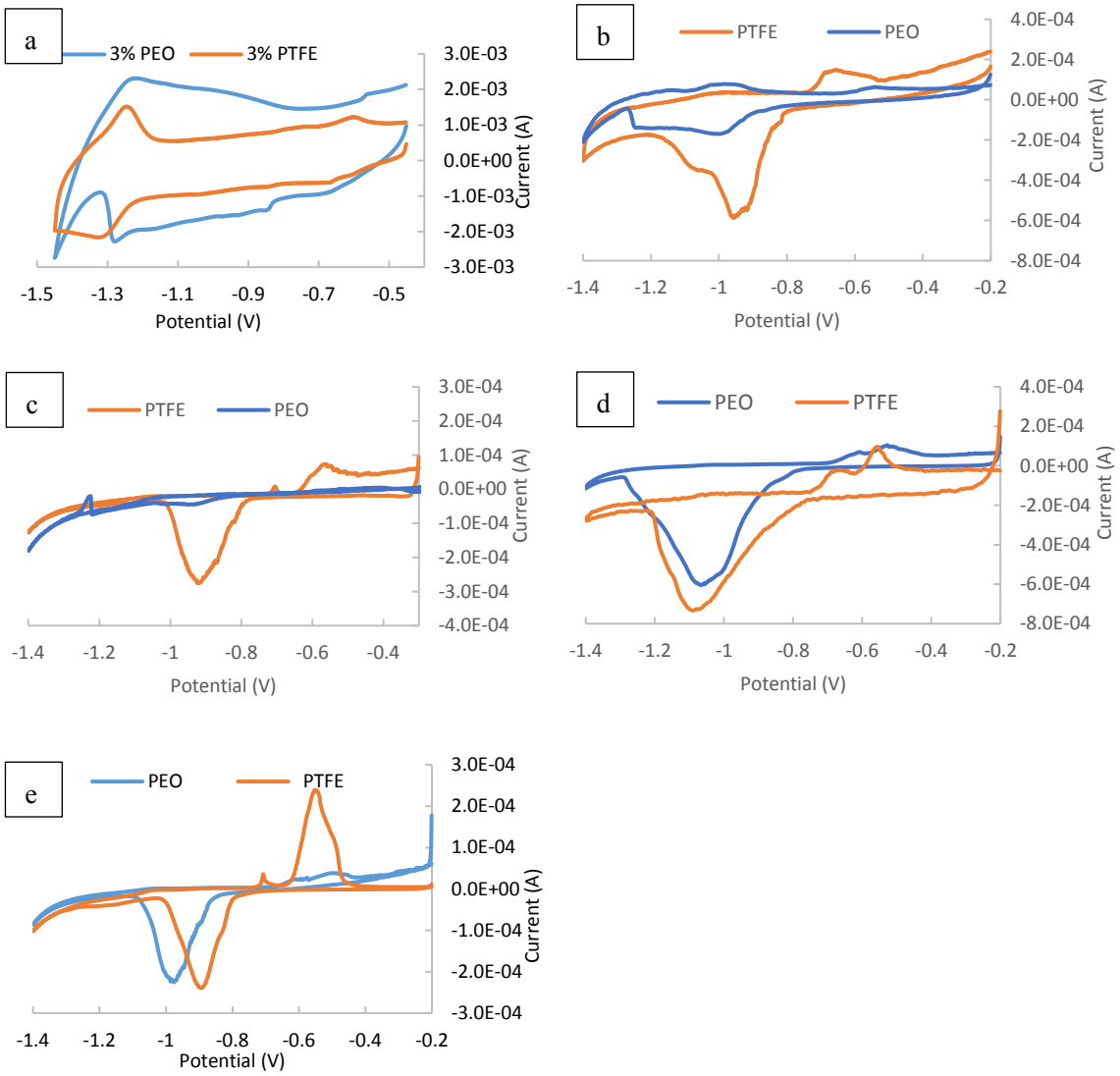

Figure 2.6 Cyclic voltammetry of anode with 3% PTFE or PEO: a) regular zinc at 100 mV/s, b) 10 mV/s scan rate, regular zinc, c) regular zinc at 0.5 mV/s scan rate, d) micron grade zinc at 1 mV/s, e) micron grade zinc at 0.5 mV/s.

The membrane maintained high ionic conductivity and stability and resisted attack from the KOH. The single layer of thin hydrophilic PTFE separator could be penetrated

with dendrites from the anode side, so another layer of glass fiber separator was employed on the cathode side. At the same time, the glass fiber worked as a partial separator and a proper medium for small amount electrolyte storage. The combined separator maintained its own chemical and psychical stability with good flexibility. The anode also contained 4% MWCNTs, which was dispersed among micron-sized zinc and PTFE bridged the conductive particles (Figure 2.2 d).

Cyclic voltammetry was carried out to find the role of PEO and PTFE as the binders in the electrode. The results are shown in Figure 2.6. Various scan rates were tested and electrodes with PTFE showed more pronounced redox peaks than PEO. A sharp current drop could be observed between -1.2 V and -1.3 V which was attributed to the depletion of OH-, which were held by PEO molecules. Compared other studies using nano-grade particles [71, 87], the redox peaks are less obvious indicating poorer cyclability. Indicating the influence from particle size. To further prove this, zinc powder with a smaller particle size (micron grade, Figure 2.6e and **2.10**) were tested. Once again, PTFE electrodes showed better cyclability especially under low scan rates when more time was available for the ions to migrate and the reaction to take place. Notably, the PEO electrodes also showed improved electrochemical performance after micron grade zinc was used (Figure 6c&e). The larger surface provided more contact between zinc and the electrolyte mitigating the reaction inhibition caused by ion accumulation/ exhaustion. However, the smaller zinc particles were also prone to more corrosion and generated hydrogen gas. Commercial battery-grade zinc used in this research had a particle size of the order of hundreds of

microns, which had been characterized before [16]. The PTFE electrodes showed better reversibility during the CV scans without concentration polarization. This was consistent with the results obtained from the battery analyzer and OCT 3D images (Figure 2.9). The anode containing PTFE showed more stable cycles and relatively smooth surfaces compared to the anode containing PEO. Minor peaks around -0.7 V and -0.84 V were due to the additive bismuth (III) compounds [88]. PEO-KOH has lower

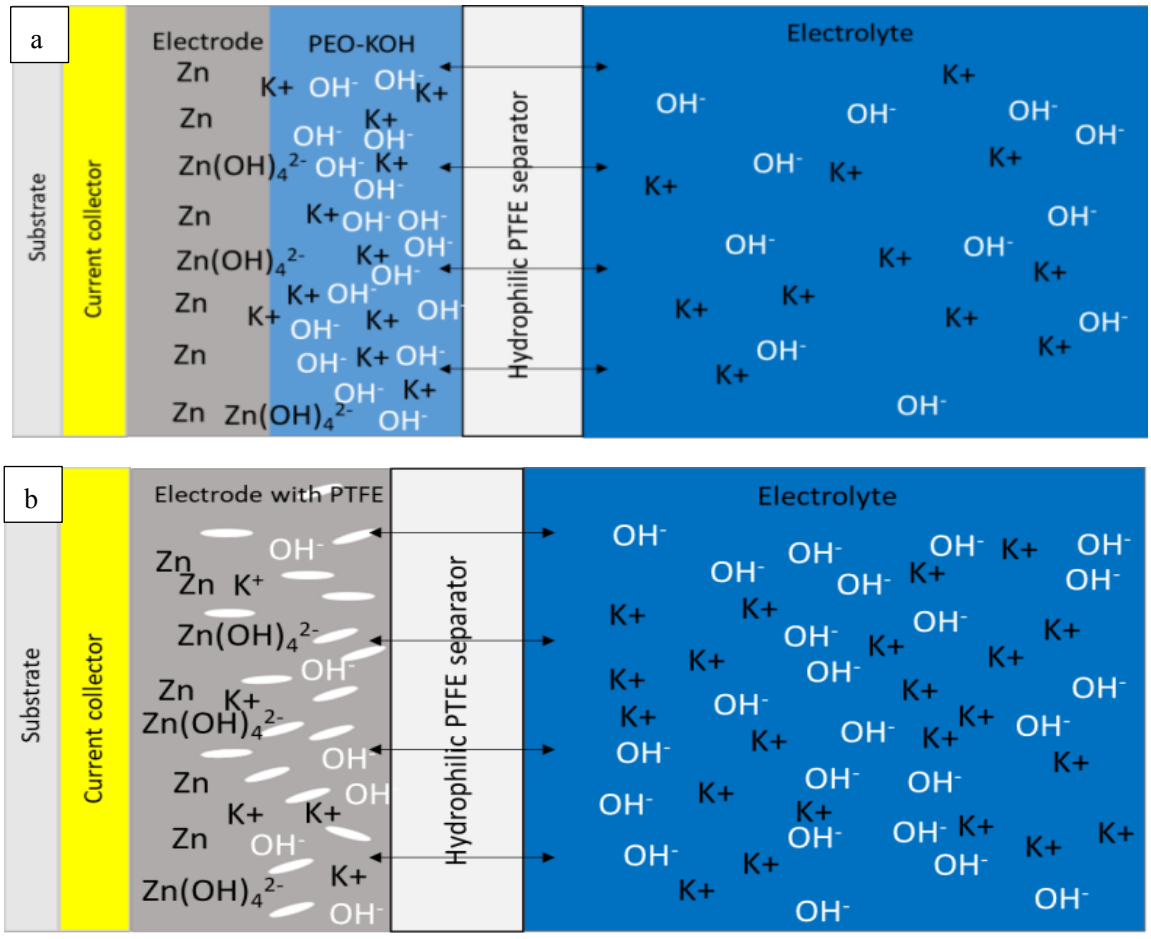

Figure 2.7 Schematic structure of electrodes with (a) PEO and (b) PTFE.

ionic conductivity (less than 3.10 ×10–5 S/cm) compared to pure water [89]. OH-

accumulated on the anode surface during the reaction (Figure 2.7), leading to relatively strong concentration polarization (around -1.3 V) and caused a sharp drop of current (Figure 2.6a). This was not observed with PTFE electrodes. Electrode with mixtures of PEO and PTFE were also tested. As the amount of PEO increased, the current drop became more pronounced (Supporting information, **Figure 2.11**). The pure PTFE electrode maintained the reversibility and showed no current drop but showed less capacitive behavior, while PEO showed poor reversibility and higher capacitance. The results from thin layer cyclic voltammetry were consistent with the performance of flexible Ni-Zn batteries, where PEO showed poor performance.

2.6. Effects of Polymer Additives and Separators

Different polymers The Swagelok and flexible cells had the open circuit voltage of 1.5 V for the first-time discharge. The performance of the flexible cell under different bending conditions is shown in Figure 2.8. Cells were bent in different bending radius: 5 cm, 10 cm and 20 cm. The flexible cells remained functional under bending although the performance was compromised.

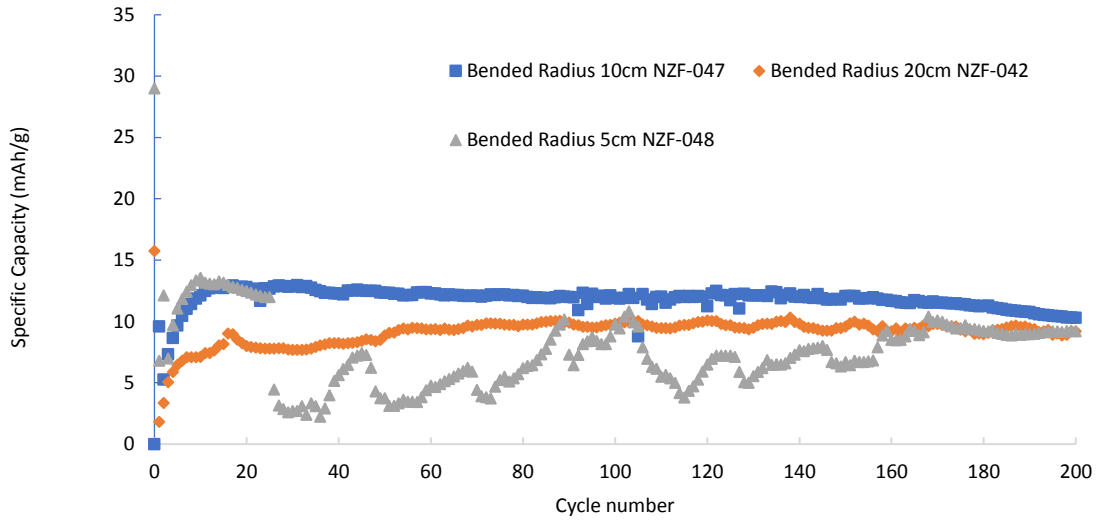

Figure 2.8 The discharge capacities of flexible cells under different bent radius conditions.

In our opinion, the performance could be further enhanced by improving the packaging of the flexible cells and optimization of electrode materials. During bending, parts of the electrodes and separator were probably stacked together while other parts lost contact. This caused fluctuations and drop in cell performance. The use of solid or gel electrolytes would avoid leakage and water evaporation and thus improve performance [90-91]. There have been several reports where metal oxides were loaded directly onto carbon material [19, 21, 68], carbon fiber cloth/ yarns [20, 71, 87, 90], or graphene [19]. Such direct loading can lead to higher conductivity and electron transfer efficiency; however, such approaches are more difficult to scale up as batteries cannot be fabricated by inexpensive printing techniques. Furthermore, reducing particle size to nano-scale could also improve capacity [69].

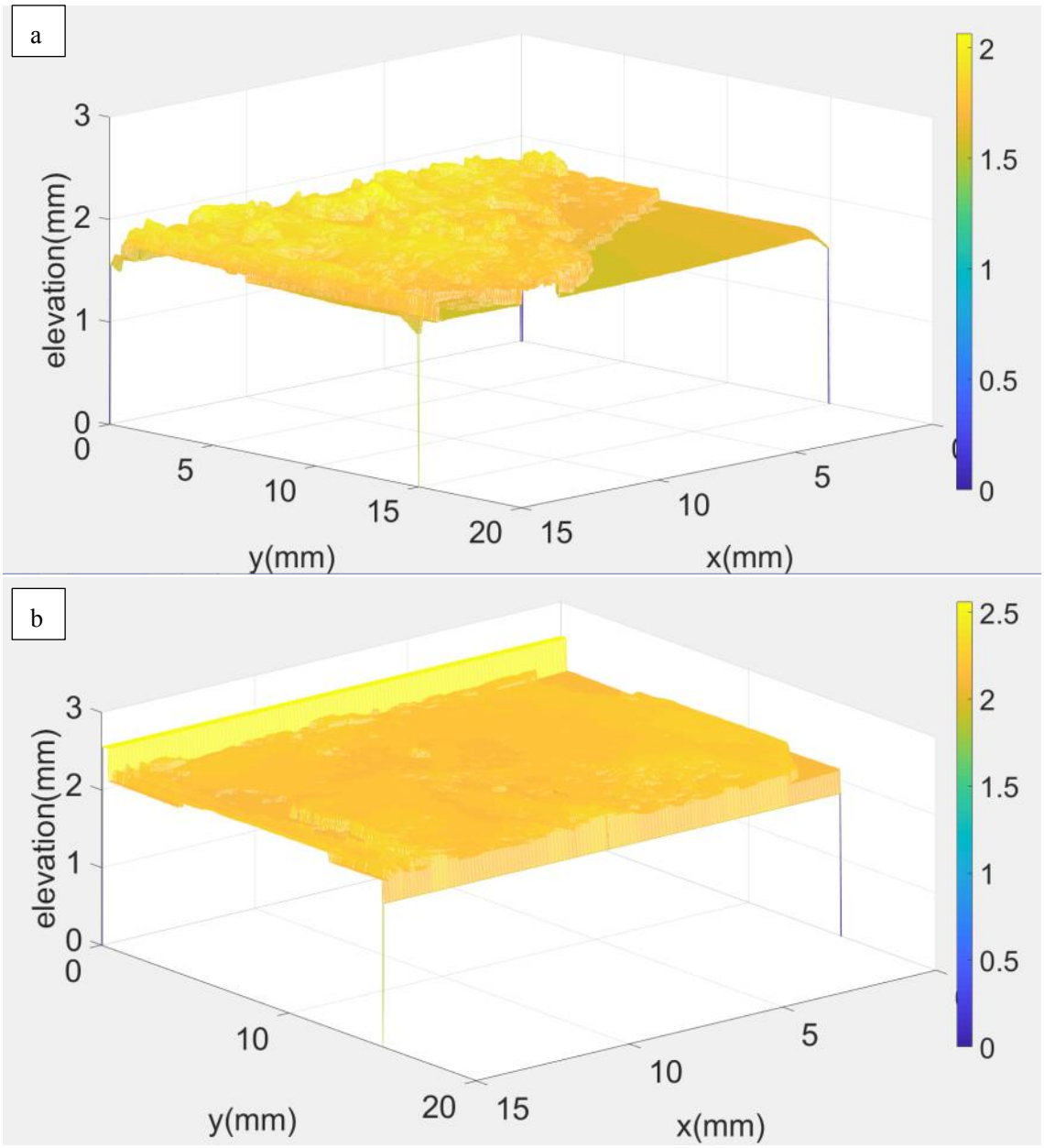

Figure 2.9 3D surface images of flexible anode for Ni-Zn cell with different polymer after cycles: (a) PEO and (b) PTFE.

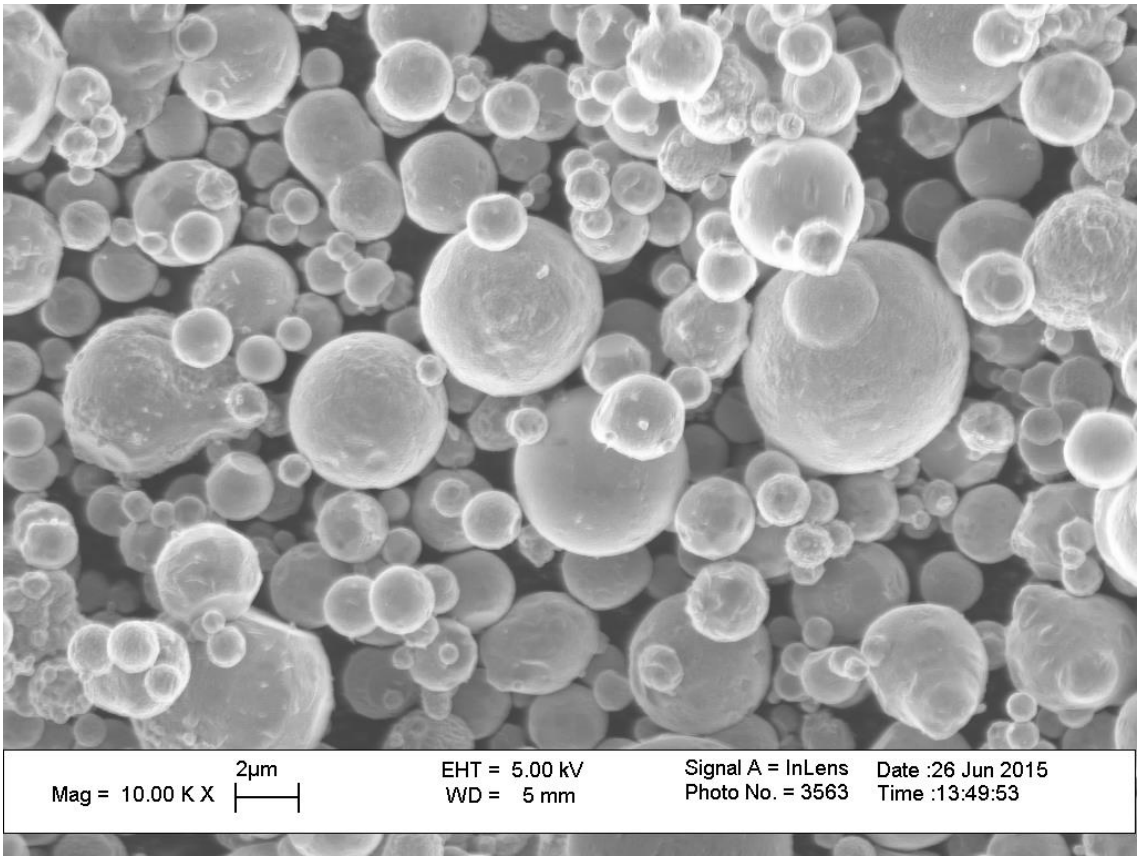

Figure 2.10 SEM image of micron-grade Zn used for cyclic voltammetry.

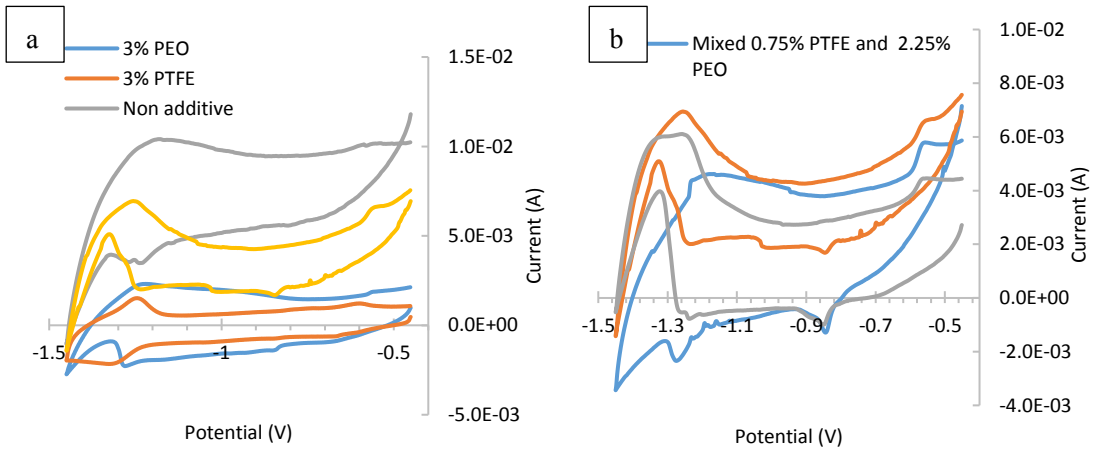

Figure 2.11 Cyclic voltammetry under 0.1 V/s scan rate for electrodes with PTFE replacing PEO as additives: (a) with and without additives, (b) mixed PEO and PTFE additives.

CHAPTER 3

FABRICATION OF PRINTABLE, FLEXIBLE NICKEL-IRON BATTERIES BASED ON CARBON NANOTUBE-METAL HYDROXIDE COMPOSITE ELECTRODES

The objective of this research is to further study and utilize the CNT implanted metal oxides. Another target is to develop flexible Ni-Fe batteries using simple, safe and inexpensive fabrication methods.

3.1 Nickel-iron Batteries

Even though the lithium ion battery currently has the highest energy density among all the chemical batteries, unsafe Li accumulation after cycles, toxic and flammable organic electrolytes keep scientists seeking more solutions on relatively safe water-based batteries. Alternates such as nickel-iron battery, originally invented around 1900 [92], has many interesting properties [93]: it endures overcharge and deep discharge during cycling; the iron electrode does not require charge state storage like lead acid battery. Compared with similar systems like Ni-Zn and Ag-Zn, Ni-Fe battery has less burden on the separators because of less significant dendrites due to low solubility of nickel and ferric oxides [94-96]. As a result, low electrode solubility is the key to provide rigid Ni-Fe battery system to have more than 30 years lifetime with some easy electrolyte refill procedures. The applications on flexible electronics, especially wearable sensors, implanted medical devices, bendable screens and smart cards [11-13], have brought more attention to Ni-Fe battery reaction because of its good

performance in long-term conditions and earth abundance of electrode materials.

3.2 Challenges of Making Flexible Nickel-iron Batteries

Various flexible batteries have been studied in recent years, including but not limited to zinc-carbon [20, 33], alkaline [18, 58, 97], metal-O_2 [16, 90, 98], nickel-iron [19, 99], nickel-zinc [14, 51, 71, 100] and lithium-ion systems [17, 21, 101]. At the same time, there are still some challenging issues to be addressed corresponding with specific electrochemical reactions. Under bending conditions, all the parts in flexible cell need to be stay in contact and kept chemically reactive. Otherwise, additives, coatings, proper design and packaging need to be applied to solve problems including dendrite formation, low electronic/ionic conductivity, and electrode disintegration [15, 102-103]. Previously reported batteries were involved with roll-to-roll printing and inkjet printing methods [104-105]. Decent electrode electric conductivity can be achieved using metallic reactants or conductive additives. The electroactive materials can be added/ deposited using various ways such as powder simply mixing, fiber weaving, dip-coating, electrochemical methods, vapor deposition [106-109]. The deposition processes vary a lot according to specific reactions and techniques. Electrodes made from chemical vapor deposition/ atomic layer deposition, and chemical bath deposition/ dip coating have good performance with high material utilization; yet such methods are also facing short-comings such as high costs, low productivity and high surface area requirements [100]. Among all flexible battery fabrication methods, aqueous phase based simple deposition of electroactive materials has the advantages on relatively high-utilized efficiency and low

cost at the same time. Typical flexible substrates for flexible batteries are hierarchical carbon cloth, nanofibers [100], cotton textile [17], nylon [97] and polyester fabrics [110]. It is also important to have proper surface areas, coatings, additives or other modification to prompt the principal reactions and inhibit undesired side reactions such as corrosion. Materials with high electrical conductivity, large surface area and chemical/ physical stability have been employed, such as graphene [19, 111-112], CNTs [21, 113], carbon microfibers [99, 114], carbon black [115], porous materials from plants [116-117] and organic conductive polymers [118].

3.3 Preparation of Metal Oxides-CNT and Active Electrode Materials

Fe_xO-CNT composites were prepared through a controlled precipitation process with NaOH and $Fe(NO_3)_3$. Certain amount of multiwall carbon nanotubes (MWCNTs, purity 95%, diameter 20-30 nm, length 10-30 μm, Cheap Tubes Inc. Brattleboro, VT, USA) was stirred in 2 M NaOH solution, before 0.1 M $Fe(NO_3)_3$ (nonahydrate, ≥98%, Sigma) solution was added into the solution at the rate of 0.8 ml min^{-1}. Then extra NaOH was removed from the composites by filtration, and composites were completely dried in a vacuum oven. The Fe_xO-CNT composites with 1:3 (CNT:Fe_xO) and 1:6 mass feeding ratio were prepared separately. Similarly, $Ni(OH)_2$-CNT was prepared by 2 M NaOH and 0.194 M $Ni(NO_3)_2$ solutions [14]. The preparation method of NiOOH cathode was described in a previous paper from our group [103]. Briefly, $Ni(OH)_2$, KOH and Clorox were mixed, stirred and heated under 60 Celsius until totally dried. Resulted sample was filtered, washed with 5% KOH solution, and dried under vacuum condition at room temperature.

3.4 Flexible Nickel-iron Cell Fabrication

The anode comprised of iron powder (Iron ≥ 99%, powder, Sigma), polymer binder, Fe_xO-CNT and multiwalled carbon nanotubes (MWCNTs). A typical dry anode contained 30% Fe_xO-CNT, 68% iron powder and 2% PTFE. Swagelok-type cells used to optimize electrode formulation, when the mass ratio of iron, iron oxide, conductive additives were varied. 5% of $Co(NO_3)_2$ were also added on anode side for tests after slurry dried on current collectors, then iron powder weight was adjusted to 63% percent.

Both $Ni(OH)_2$ and NiOOH were tested as cathode materials. The former typically contained 98% $Ni(OH)_2$-CNT and 2% PEO, while the latter contained 98% β-NiOOH and 2% PEO. The weighed electrodes materials were mixed in the DI water, and stirred to form inks. Electrodes material mixtures with precipitated metal oxides were stirred for 2 hours. The cathodes with β-NiOOH were stirred uniformly in high speed for 30 min and applied right away onto current collectors with an area of 3 cm × 2 cm. Anti-corrosion stainless steel mesh was the current collectors, then they were attached to polyethylene terephthalate (PET) layers to serve as electrode tabs. The slurries for Swagelok-type cells contain less DI water compared with the ink for flexible cells. After the inks/slurries were applied onto the current collectors, the electrodes were dried at room temperature slowly in fume hoods for 6 hr. The being studied electrodes were always the limiting reagent, which was 0.036 g, with the other side electrode weight 10% more in stoichiometry. The electrolyte was 6 M KOH (sigma), sometimes saturated with LiOH whereas mentioned.

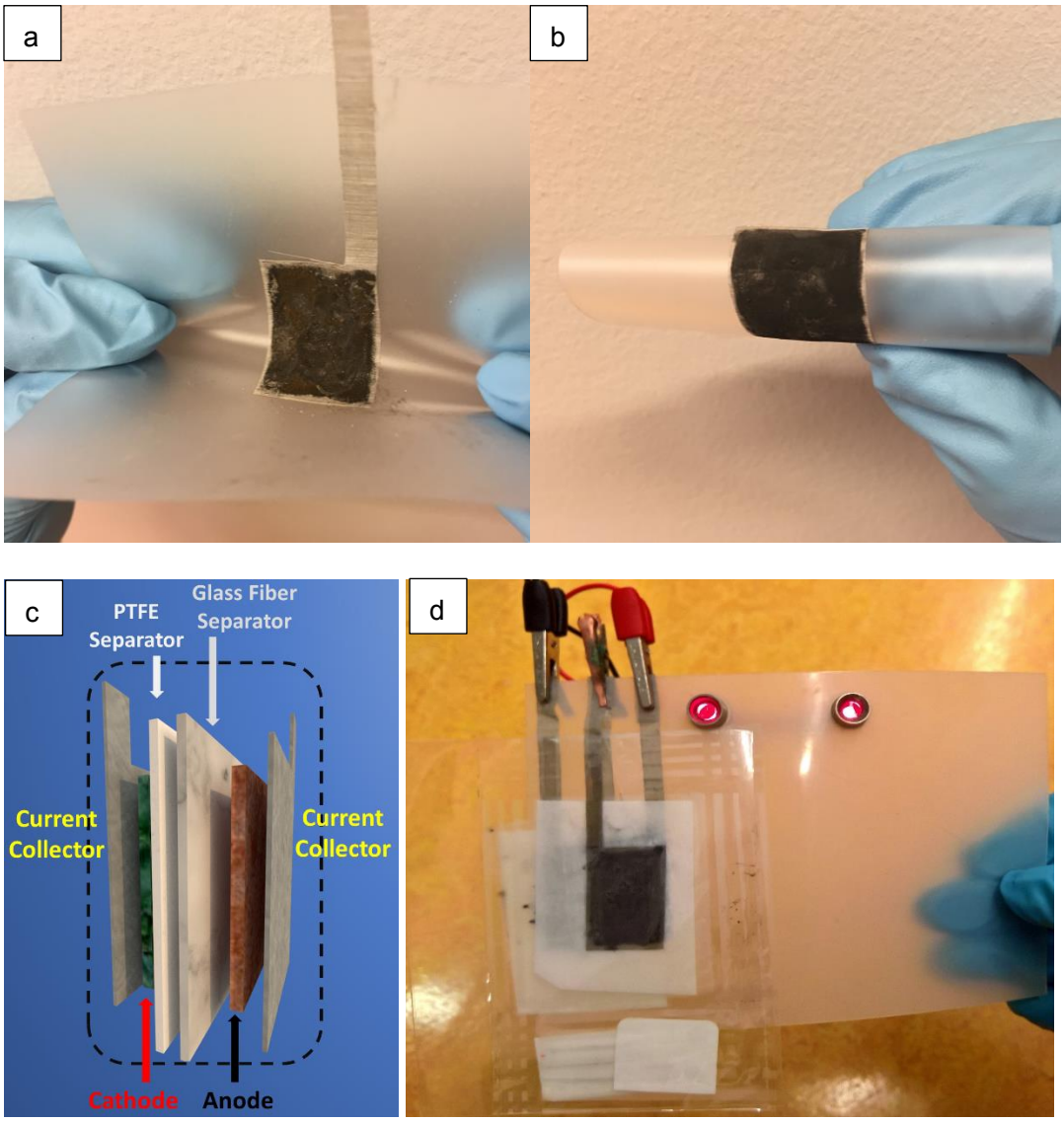

Figure 3.1 (a) flexible anode; (b) flexible cathode; (c) Structure of a flexible secondary Ni-Fe battery. (d) LED lights powered by two flexible Ni-Fe battery

Anti-corrosion stainless steel 304 mesh (wire diameters 0.1651 mm and 0.03556 mm, 31% open area) were used as current collectors. Glass Fiber (Whatman, Grade GF/A 1.6µm), hydrophilic PTFE (Hangzhou ANOW Microfiltration, pore size 5µm) separators and their combinations were tested in this flexible battery model individually. In a flexible

cell, all layers were sandwiched as shown in **Figure 3.1c** and thermally sealed.

3.5 Materials Characterization for Flexible Nickel-iron Cells

Scanning electron microscope (SEM) images were collected on a LEO 1530 VP Scanning Electron Microscope. X-ray powder diffraction (XRD) patterns were taken on Philips, EMPYREAN. Thermal gravity analysis (TGA) was done on PerkinElmer Pyris 1. The electrochemical performances of the cells were measured by discharging and charging them under constant current modes using an MTI Battery Analyzer (Richmond, CA). Electrode was used to study electrochemical properties. The working electrodes (5 mm × 2 mm) had smaller surface area than the platinum counter electrode. The electrode was prepared in the same way as flexible battery electrodes; and then a hydrophilic PTFE membrane was thermally laminated to fortify the electrode layer. Typical mass of the thin-layer working electrode for cyclic voltammetry was 0.005g after drying.

3.6 Optimization of Flexible Nickel-iron Cells

3.6.1 Active Electrochemical Materials and MWCNTs Implanted Materials

Figure 3.1a is the photographs of metal oxide-CNT inks. 2b shows the flexible electrodes under bended conditions respectively. Structure of the layered flexible battery is shown in Figure 3.1c. The flexible separator combination has a hydrophilic PTFE on the cathode side and glass microfiber on the anode side. Figure 3.2 presents the SEM images of Fe_xO-CNT, $Ni(OH)_2$-CNT and β-NiOOH. Carbon nanotubes can be seen imbedded inside

electroactive material related to the formation of conductive networks.

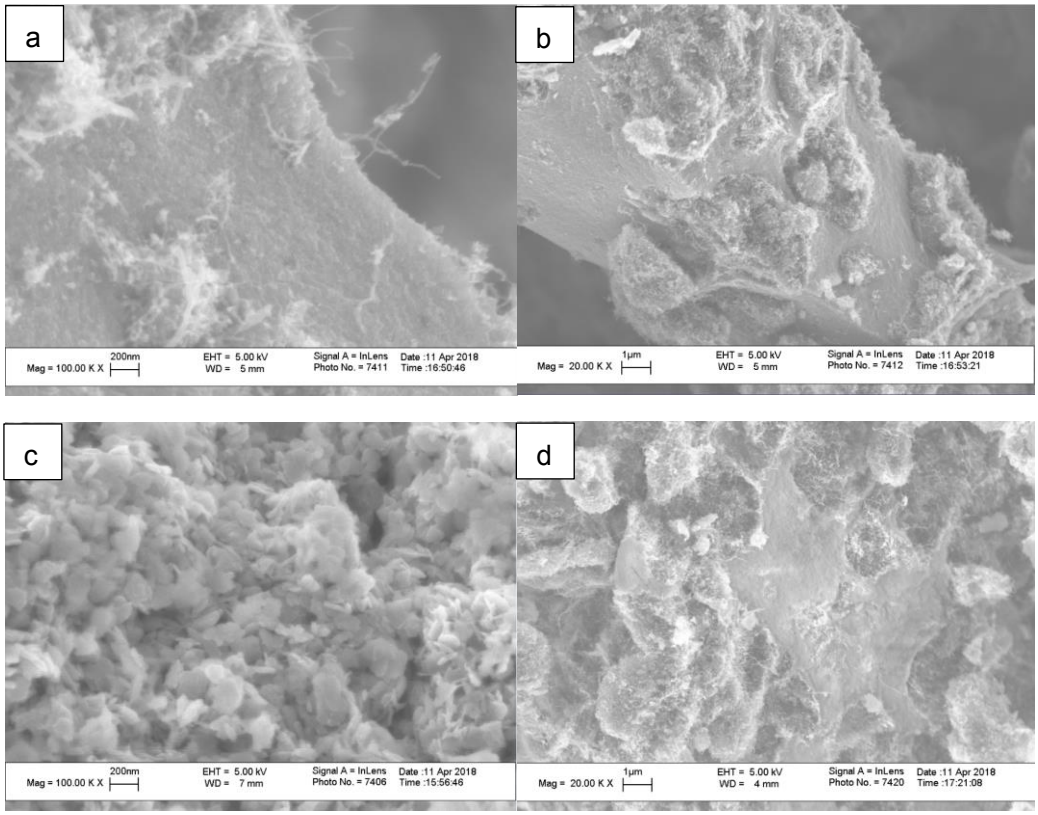

Figure 3.2 (a) and (b) SEM images of Fe_xO-CNT, (c) β-NiOOH (d) $Ni(OH)_2$-CNT

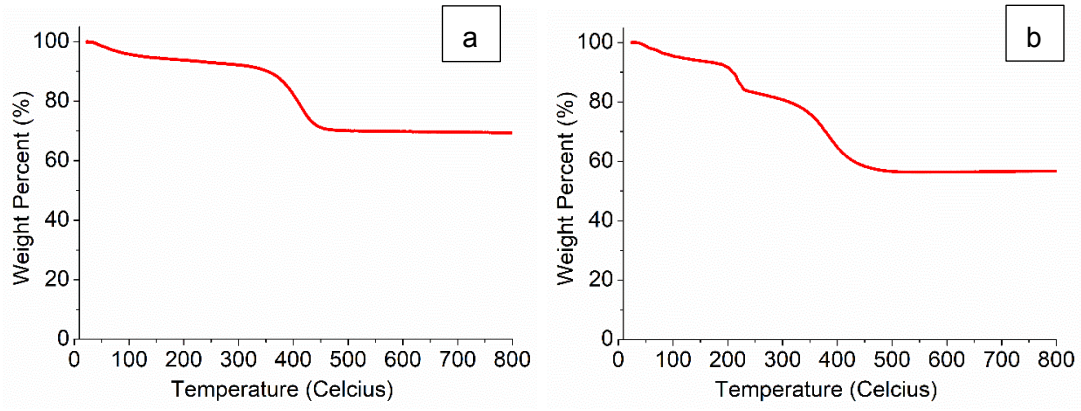

Figure 3.3 TGA of (a) Fe_xO-CNT 3:1 (feeding ratio) and (b) $Ni(OH)_2$-CNT 3:1

Nickel hydroxides and nickel oxides have relatively poor electrical conductivity. The metal hydroxides implanted with MWCNTs solved this kind of problems. The preparation and optimization procedures of $Ni(OH)_2$-CNT composites were described in a paper from our

group previously. Based on previous studies, the best performing $Ni(OH)_2$-$CNT_{29.7}$ was used directly for this flexible nickel-iron system [14]. The overall XRD pattern of $Ni(OH)_2$-CNT showed amorphous shape as shown in **Figure 3.8**. It did not represent any specific identical peaks of nickel hydroxides or nickel oxides like reported elsewhere [119]. Simple mixing of commercial $Ni(OH)_2$ with CNTs were also tested yet yielded very poor performance.

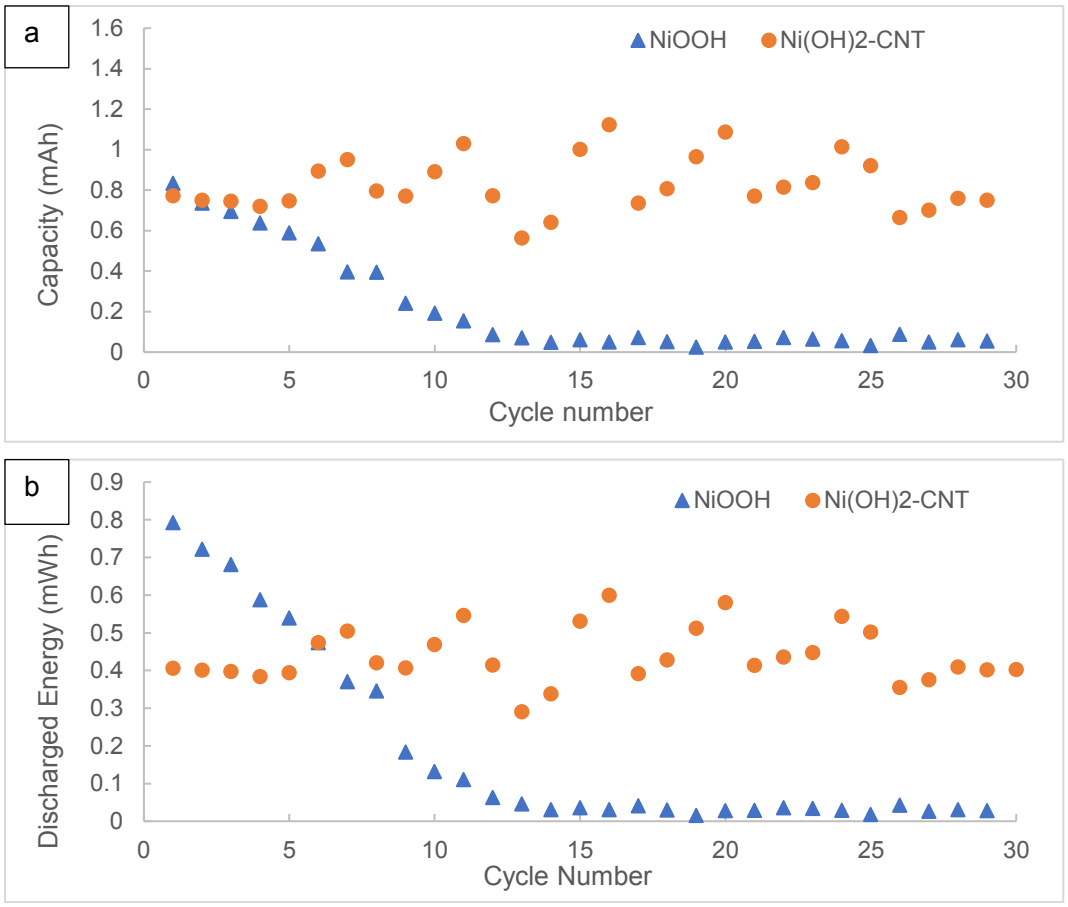

Figure 3.4 Discharge (a) capacity and (b) energy of different cathode materials in Swagelok cells.

Figure 3.4 showed that $Ni(OH)_2$-$CNT_{29.8}$ brought higher discharge capacity and more stable discharge energy than β-NiOOH by using the same method. $Ni(OH)_2$-CNT has

the ideal conductive high surface area MWCNT network inside the active reactants.

Ni-Fe battery has two reactions:

$$\text{Reaction 1: } Fe + 2NiOOH + 2H_2O \rightleftharpoons Fe(OH)_2 + 2Ni(OH)_2$$

$$\text{Reaction 2: } 3Fe(OH)_2 + 2NiOOH \rightleftharpoons Fe_3O_4 + 2Ni(OH)_2 + 2H_2O$$

In tested Ni-Fe cells, β-NiOOH provided the stable discharge plateau around 1.2 V. (**Figure 3.9**), favoring 1st reaction. Yet the stability of β-NiOOH turned out to be lower compared with $Ni(OH)_2$-CNT.

The Fe_xO in the anode was also loaded onto CNTs via co-precipitation to form a composite as shown in **Figure 3.2a and b**. A reaction between $Fe(NO_3)_3$ and NaOH was used to synthesize $Fe(OH)_3$, which was then dehydrated to Fe_xO by heating at 200 ℃ overnight. The EDX results from the final composite showed the presence of Fe, C and O. The concentration of Fe_xO in the composite could be varied by varying the amount of the reactants during precipitation. Anodes tended to crack at high CNT concentration and during bending when all of the composites are simply mixed. This has also been reported before [18]. Compared with simple mixing of ferric oxide and MWCNTs, incorporating MWCNTs into Fe_xO prevented electrode cracking with slow room temperature drying process. After the TGA test, the actual composition of the working Fe_xO-$CNT_{25.7}$ (3:1 feeding ratio) has 70% Fe_2O_3, 25.7% CNTs and 4.3% H_2O. The major drop at 400 Celsius was due to the burning of CNTs. A similar drop was also observed in the $Ni(OH)_2$-CNT composite, which was calculated to contain 29.7% CNTs. The drop before 200 Celsius was

attributed to removal of adsorbed and crystalline water, as well as the decomposition of $Ni(OH)_2$ to NiO. XRD pattern of Fe_xO-CNT and $Ni(OH)_2$-CNT were shown in Figure. 3.8. No obvious peaks were observed even when the scanning speed was low. Possibly, because of the existence of large amount of CNTs, the composites showed amorphous rather than crystalline structure.

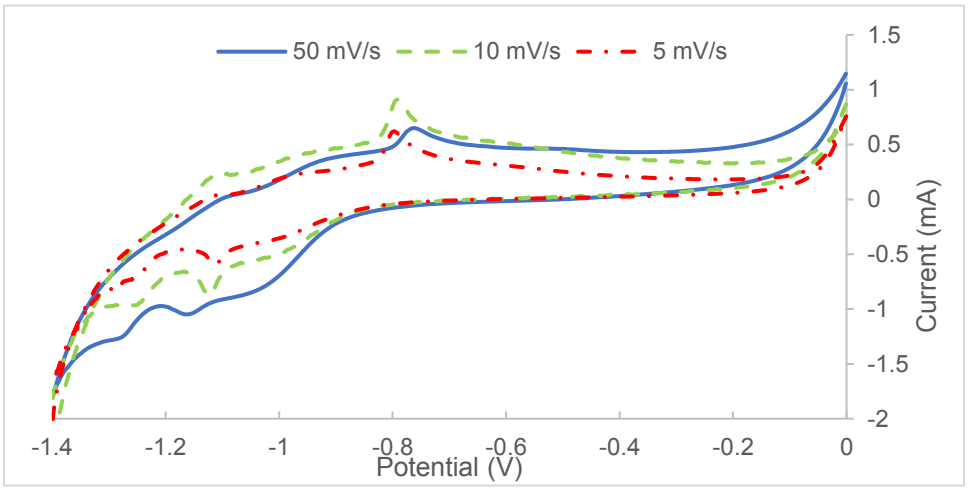

Figure 3.5 Cyclic voltammetry of anode paste with Fe_xO-$CNT_{25.7}$ (3:1 feeding ratio)

Cyclic voltammetry analysis of Fe_xO-CNT composites showed the conversion among Fe, Fe(II) and Fe(III) in **Figure 3.5**. Oxidation peaks were always shown around -1.13 V and -0.78 V, the latter more prominent. Reduction peaks were appeared around -1.33 V and -1.16 V. Significant hydrogen evolution was observed at the lower potential end.

These Fe_xO-CNT composites were used to make anodes for nickel-iron cells. Proper ratio of iron powder was added to anode to benefit the cycling performance. The charge-discharge method was as this: charging at 4 mA current for 120 min; then cell was

discharged at 0.2 mA to 0.4 V. Composites with different CNT percentages were also tested. Fe_xO-$CNT_{25.7}$ with 25% CNT feeding showed decent electrochemical performance. Fe_xO-CNT with 6:1 ferric oxide:CNT feeding ratio could hardly be charged, possibly due to the high electric resistance. Higher percentage of MWCNTs would greatly increase the ink viscosity as well as cracking during drying process, and decrease the amount of active materials.

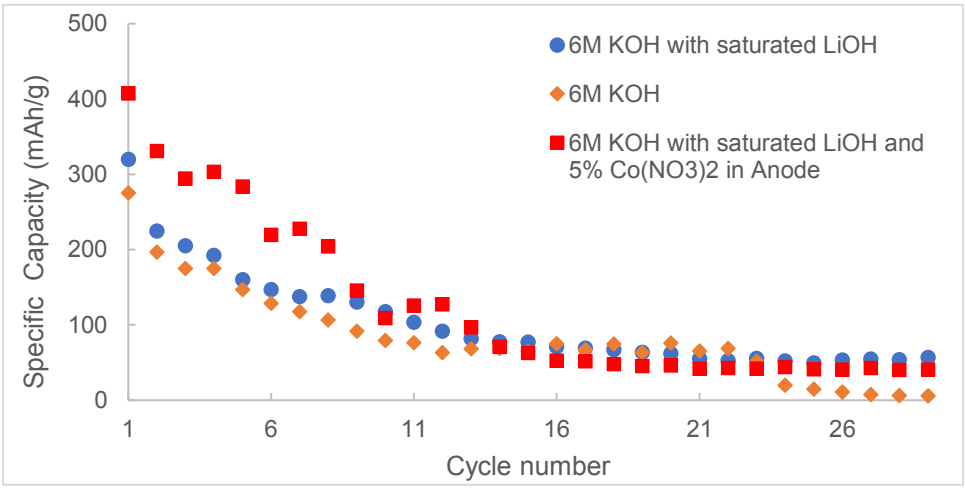

Figure 3.6 Flexible Ni-Fe cell performance with different electrolytes and composition using NiOOH cathode and Fe_xO-$CNT_{25.7}$ anode

3.6.2 Effects of LiOH in Electrolytes and $Co(NO_3)_2$ on Anode

Other modifications also benefited the performance of flexible nickel-iron cells as shown in **Figure 3.6**: introduction of α-$Co(OH)_2$ in the anode and using 6 M KOH saturated with LiOH improved cell performance. The presence of α-$Co(OH)_2$ improved conductivity and consequently cell performance [120], and at the same time, the conversion between Co(II) and Co metal could benefit the electrode rechargeability [121]. It is also believed that the small diameter lithium ions led to the formation of $Li_xFe_yO_z$ intercalation-compounds,

which helped its further reduction to iron metal and improved overall cell performance [122]. Lithium also decreased the carbonate content in electrolyte since Li_2CO_3 solubility was much lower than that of K_2CO_3, thus decreasing the amount of CO_3^{2-} in electrolyte and protecting the cathode [123]

3.7 Flexible Nickel-iron Cell Performance

The Swagelok and flexible cells had the initial voltage of 1.2 V and open circuit voltage of 1.4 V after the first-time charging. The performance of the flexible cell under different bending conditions is shown in **Figure 3.7**. Flat cells were bent at different radius: 4 cm, 8cm. The flexible cells remained functional under bending although the performance was compromised. When bent, parts of the electrodes and separator were stacked together while other parts lost contact, causing voltage fluctuations and a drop in cell performance. Performance could be further improved by having better internal contacts, electrolyte storage and more advanced packaging.

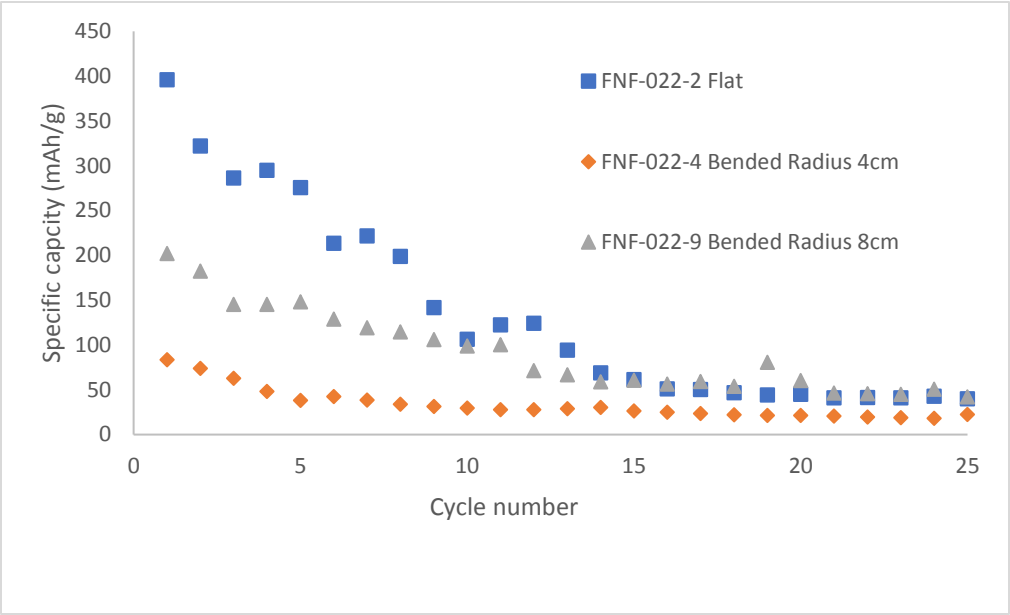

Figure 3.7 The discharge capacities of flexible cells under different bended radius conditions.

Compared to the co-precipitated Ni-Fe battery presented here, the Ni-Zn battery made by a somewhat similar approach [103] showed lower specific capacity. This was attributed to the higher stability of iron compared with zinc electrodes. It is known that zinc oxide dissolves in alkaline to form zincates. The dynamic equilibrium between zincates and zinc oxide, as well as the charge-discharge process change the morphology of zinc anode so that additives had to be added to inhibit such processes [63, 103]. This type of transformation on zinc electrodes does not take place the same way on iron electrode surfaces, as Fe_2O_3 is more stable and insoluble in alkaline environment. The iron oxides/hydroxides redox follows a relatively slow two-step process which leads to higher material utilization; the low solubilities of iron hydroxides and iron oxides define the small and low concentration diffusive layer of iron related active materials. Zinc corrosion is another problem encountered with Zn electrodes where the hydrogen produced

compromises battery performance [41, 124]. These problems are not encountered in an iron electrode which is more stable [125]. These allow the battery to be stored for longer periods.

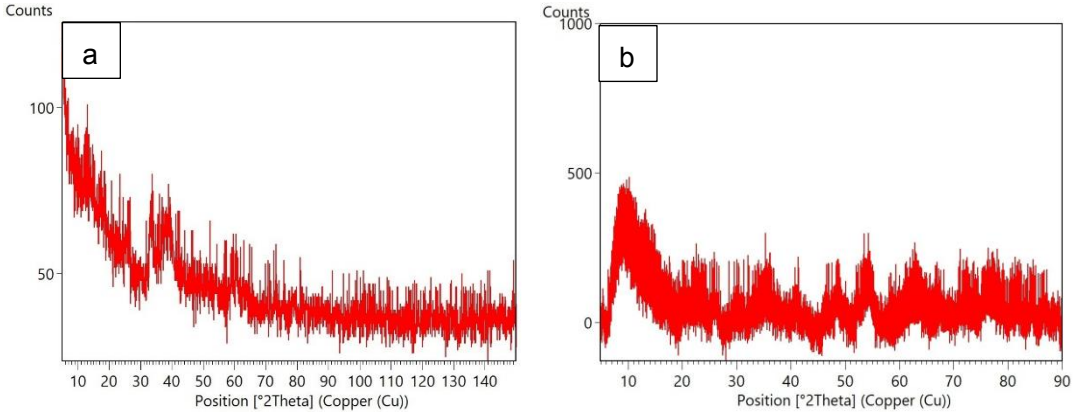

Figure 3.8 XRD of pretreated (a) Ni(OH)2-CNT and (b) FexO-CNT.

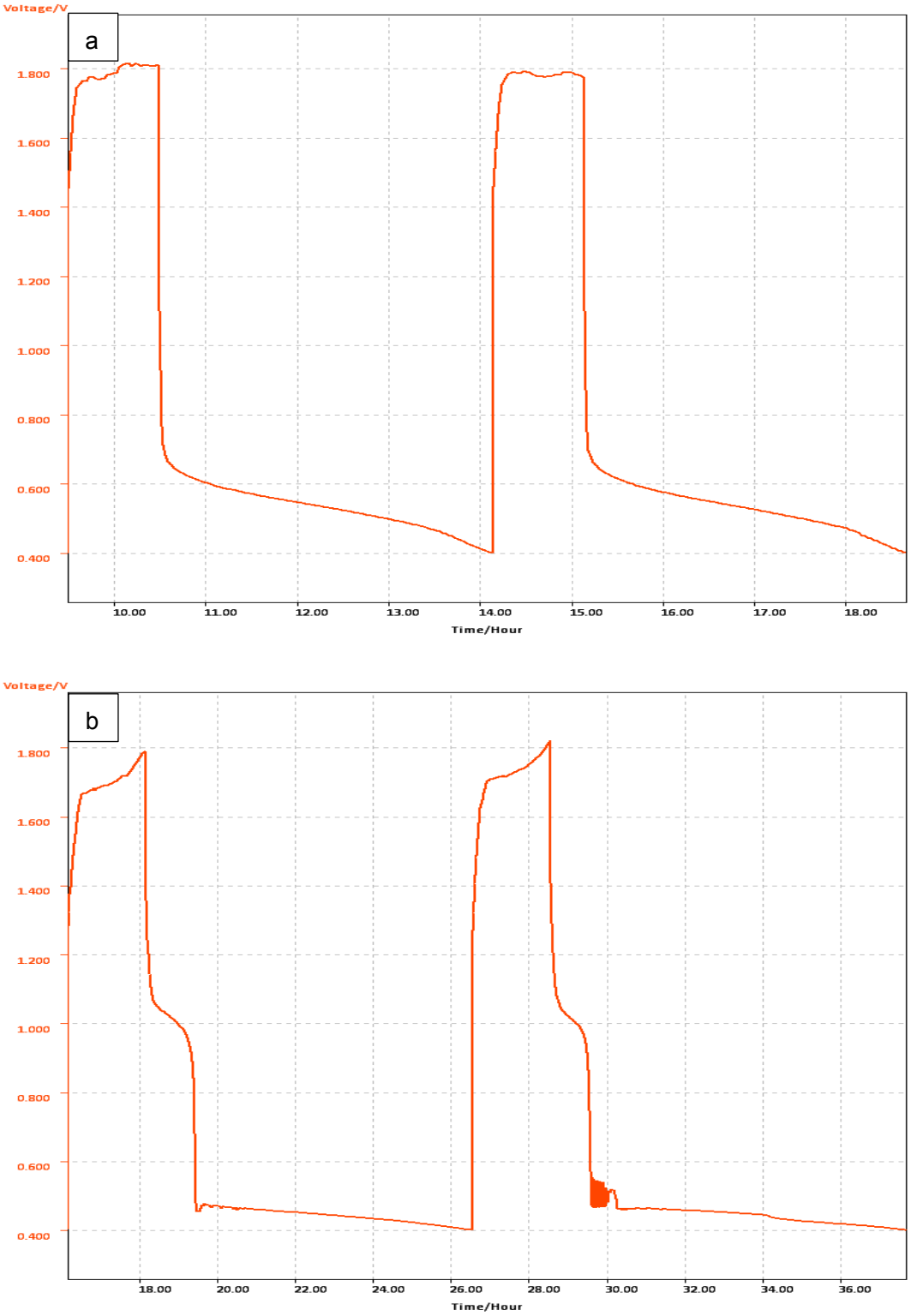

Figure 3.9 Discharge voltage graph of (a)NiOOH in Swagelok cell (b) $Ni(OH)_2$-CNT in Swagelok cell.

CHAPTER 4

DEVELOPMENT OF NICKEL IRON ROPE/CABLE BATTERY WITH IRON OXIDE CARBONNANOTUBE RESERVE ELECTRODES

After the development of metal oxide-CNT composites, the aim of this research is to utilize the them for rope shape battery by simple painting methods.

4.1 Rope Batteries and Suitable Applications

The first mature rope battery design came out on 1985 [126], the inventor claimed the design is for high voltage, long working time and relative low cost by activation using fresh, salt water and other electrolytic medium. By using fiber-shape active materials and membrane separator, another type of fibrous battery cell was invented in1995 which could also be packed into rope shape batteries[127]. The shape advantage of rope and flexible batteries improved their adaptivity, so they could have more chances to wrap around or attach to the surface, to insert into the empty part of the applications without changing their main functions. The potential circumstances would substitute some of the package, connection or physical supporting parts. Other than the applications on short or long cable surfaces, these batteries are also appropriate for sensor carriers sending to somewhere unsuitable for human operation. Typical applications would be gas controlled robots and snake robot fire extinguishing and signaling [128]. Recently, the prominent skin controlling robots [129] are also suitable for cable batteries when they are directly combined with controlling skin in the future, so the power source need not to be supplied that much from outside.

4.2 Challenges On Rope/Cable Battery

Like the previous chapters mentioned, many electrochemical systems including but not limited to zinc-carbon [20, 33], alkaline [18, 58, 97], metal-O_2 [16, 90, 98], nickel-iron [19, 99], nickel-zinc [14, 51, 71, 100] and lithium-ion systems [17, 21, 101] have been studied for fabrication of flexible battery models. Other than under bending conditions, rope/cable battery also need to maintain all the parts in contact and active on much longer shape applications. Good performance in terms of capacity, energy, working voltage and cycle stability under challenging conditions are desired. As a result, the selection of proper chemical reaction is important for cable battery to meet these requirements. In the description of this designed rope patent in 1985 [126], the inventor not only claimed to be comprehensive on primary and secondary batteries, but also covered usage or selective usage of elements like magnesium, aluminum, zinc, lead, silver, platinum, palladium, ruthenium, nickel and alloys thereof，but low cost and safe iron was not listed in the design. The fibrous cell design [127] invested more efforts on micro level structure of electrodes; however, the specific volumetric power density would be decreased by using many layers of membrane separators packed in cells. Considering applicable situations, nickel-iron battery is still a proper candidate for rope/cable batteries application with its advantages: extremely long shelf lives with life maintenance, durability under regular using and special conditions, including overcharge, over-discharge, short circuit, overheating and resistance to shock/vibration [1, 94].

4.3 Design and Fabrication of Metal Oxides-CNT Based Rope Battery

4.3.1 Electrode Materials Selection

For nickel-iron rope/cable battery, Fe_xO-$CNT_{25.7}$ composites were produced through a controlled precipitated process with NaOH, $Fe(NO_3)_3$ mentioned in chapter 3. β-NiOOH cathode active material was described in a previous paper from our group [103]. The electrolyte was 6M KOH (Sigma) with saturated LiOH.

To evaluate the rope battery model, same compound ratio simply mixed nickel-iron and nickel-zinc rope battery without metal oxides precipitated composites.

4.3.2 Production of Reserve Electrodes and Rope Battery

In nickel-iron composite rope battery, the anode comprised of iron powder (Iron ≥ 99%, powder, Sigma), polymer binder, Fe_xO-$CNT_{25.7}$ and multiwalled carbon nanotubes (MWCNTs). The dry composite iron anode contained 30% Fe_xO-$CNT_{25.7}$, which was optimized in chapter 2, 68% iron powder and 2% PTFE. In nickel-iron mixture rope battery, anode formulation is 23% Fe_2O_3, 7% CNT, 68% iron powder and 2% PTFE. In nickel-zinc mixture rope battery, the dry mixture anode was 20% ZnO (Sigma), 7% CNTs, 68% zinc powder 3% Bi_2O_3 and 2% PTFE.

The cathode formulation is 98% β-NiOOH and 2% PEO for all these three rope batteries. Anode formulations need to be physically stirred for at least 1 hour to form stable mixture slurry. The cathode β-NiOOH must be stirred with high speed magnetic stirrer for 30mins and applied to the surface of anti-corrosion 304 stainless steel mesh current

collector right away. The electrodes especially the cathode with Ni(III) had to be dried at room temperature slowly in fume hoods for 6 hr. In this research, anodes were still 0.04 g as the limiting reagents, and NiOOH cathode weight is 30% more stoichiometrically. For a single reserved electrode, a layer of polyethylene terephthalate (PET) with ethylene vinyl acetate (EVA) coating inside were serving as the inner spring and current collector holding sheet at the same time. After drying process of active materials on the current collector, only one layer of the whole 2mm* 11cm strip with active material were thermally sealed in between the PET-EVA copolymer sheet and hydrophilic modified PTFE membrane (Hangzhou ANOW Microfiltration, pore size 5μm). One-layer active material, which was different from commonly used rigid battery stacked cells, was to assess the difference on formulations.

To assemble the whole rope battery, anode and cathode reserved electrodes were attached together with a layer of proper size glass fiber separator, which also can store electrolyte, in the middle. The whole set can be twisted to form a helix, after adding the electrolyte, then they could be either thermally sealed together inside a package, or on the surface of a cable to have a rope shape. Nonconductive liquid tape (Performix LT14023) was also applied to the ending sites when needed.

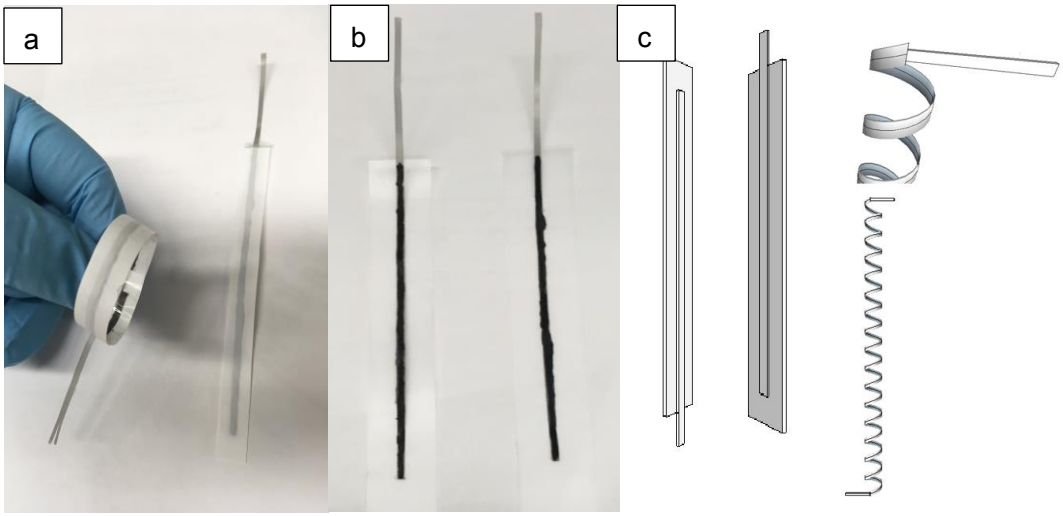

Figure 4.1 (a) flexible reserved electrodes; (b) flexible electrodes before laminating; (c) Structure of a flexible rechargeable Ni-Fe rope/cable battery.

4.4 Flexible Rope Nickel-iron Cell Performance

After at least one fully charged step, the Ni-Fe rope battery open-circuit voltage level was around 1.4 V for the first-time discharge, and Ni-Zn rope cells had 1.5 V open-circuit voltage. All the cell performances were checked with MTI Battery Analyzer (Richmond, CA). Ni-Zn cells **In Figure 4.3**, Ni-Fe rope battery with reserved electrodes with precipitated FexO-$CNT_{25.7}$ had more than 90mAh/g specific discharge capacity under straight condition and 60mAh/g with 8cm bent radius condition. The bended Ni-Fe cell result is sensible because under bending condition it was challenging the contact of each parts in the same cell. The Ni-Fe rope cell using simple mixing method with the same compound ratio only had a 40mAh/g level discharged capacity, probably due to less wicking and surface area effect without coated CNTs.

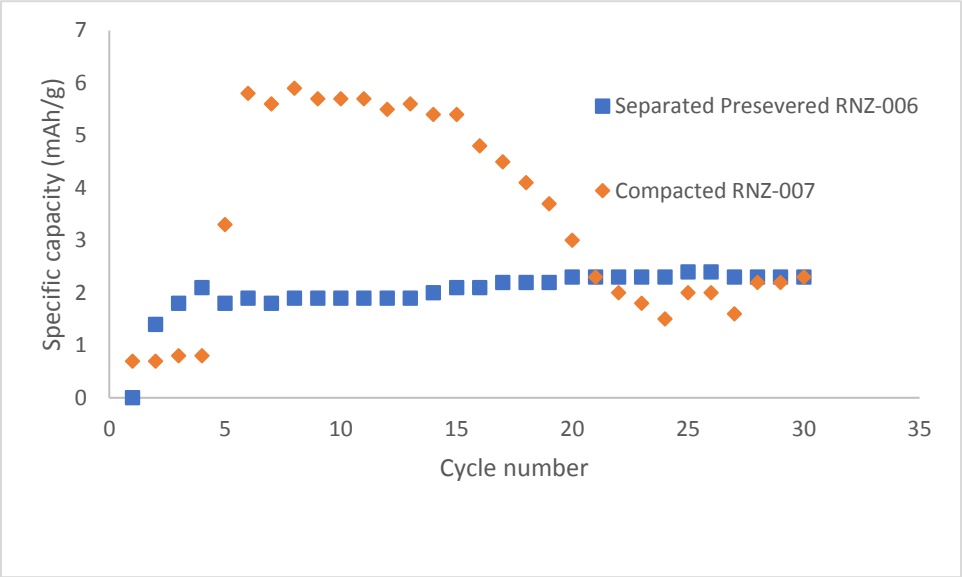

Figure 4.2 The discharge capacities of Ni-Zn rope cells with reserved electrode packing method and direct lamination method.

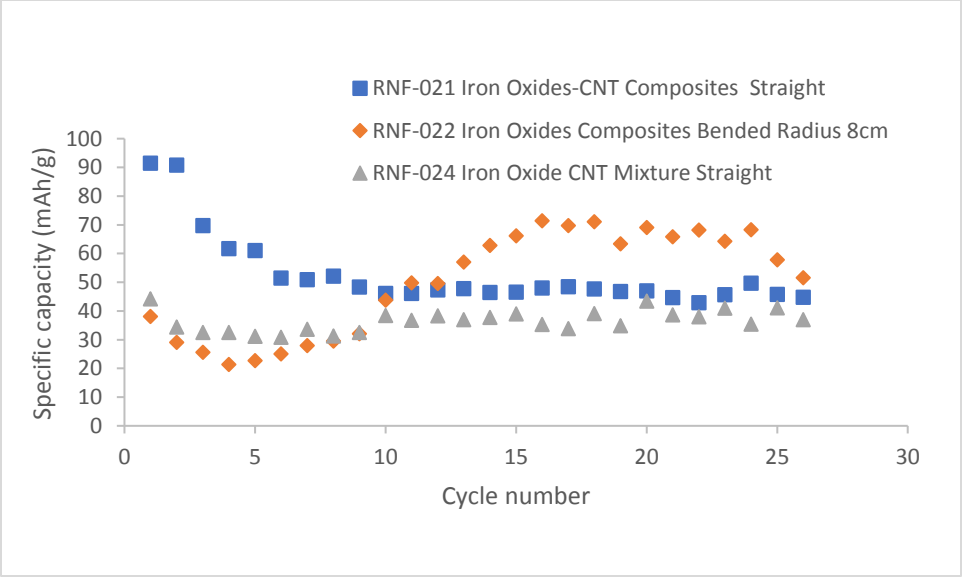

Figure 4.3 The discharge capacities of Ni-Fe rope cells under different straight and bended conditions.

CHAPTER 5
CONCLUSIONS

The development of simple, flexible Ni-Zn batteries where the electrodes were synthesized via facile mixing of electrode slurry was showed. Charge-discharge stability was improved by using PTFE as a binding material in the anode. Detailed cyclic voltammetry showed that PTFE did not introduce concentration polarization which was observed in the case of PEO. Additionally, PTFE did not change zinc electrode morphology like PEO did after long-time cycling. This makes PTFE an attractive material for flexible electrode fabrication.

Paintable nickel-iron flexible batteries and their production processes were presented. Fe_xO-$CNT_{25.7}$ provided proper amount of high surface area MWCNT conductive network avoiding cracking during bending process. Compared with β-NiOOH, $Ni(OH)_2$-CNT ensured better cycling stability for higher capacity in cells. β-NiOOH provided more stable discharge plateau than $Ni(OH)_2$-CNT at around 1.1 V. For the initial cycles, a high specific capacity of 331 mAh g^{-1} was achieved by introduction of blue layer structured α-$Co(OH)_2$ on anode side and 6M KOH electrolyte saturated with LiOH, even when the cells were over charged and discharged.

Ni-Fe and Ni-Zn rope batteries of the same dimensions were fabricated using the same method (except anode formulation) and tested on the battery analyzer. Ni-Fe rope battery with reserved precipitated FexO-$CNT_{25.7}$ electrodes (90mAh/g straight and 60mAh/g with 8cm bended radius) showed better discharge capacity than Ni-Fe cell using

mixed Fe_2O_3 electrodes (40mAh/g) and Ni-Zn cell with mixed ZnO and CNTs. Therefore, rope/cable battery model is more suitable for less soluble Fe_2O_3-CNT composite electrodes than zinc electrodes.

REFERENCES

1. Reddy, T., Linden's Handbook of Batteries. In *By Thomas B. Reddy. 4th Ed. Mcgraw-Hill*, 2011.

2. Kang, F.; Chengjun, X.; Li, B.; Hongda, D., Rechargeable Zinc Ion Battery. US Patent 8,663,844, 2014 2014.

3. Wu, M.; Zhao, T.; Jiang, H.; Zeng, Y.; Ren, Y., High-performance Zinc Bromine Flow Battery Via Improved Design of Electrolyte and Electrode. *Journal of Power Sources* **2017,** *355*, 62-68.

4. Wang, Z.; Meng, X.; Chen, K.; Mitra, S., Development of High Capacity Periodate Battery with 3D-printed Casing Accommodating Replaceable, Flexible Electrodes. *ACS Applied Materials & Interfaces* **2018**.

5. Pan, H.; Shao, Y.; Yan, P.; Cheng, Y.; Han, K. S.; Nie, Z.; Wang, C.; Yang, J.; Li, X.; Bhattacharya, P., Reversible Aqueous Zinc/Manganese Oxide Energy Storage from Conversion Reactions. *Nature Energy* **2016,** *1* (5), 16039.

6. McKerracher, R.; Ponce de Leon, C.; Wills, R.; Shah, A.; Walsh, F. C., A Review of the Iron–air Secondary Battery for Energy Storage. *ChemPlusChem* **2015,** *80* (2), 323-335.

7. Padhi, A.; Nanjundaswamy, K.; Masquelier, C.; Okada, S.; Goodenough, J., Effect of Structure on the Fe^{3+}/Fe^{2+} Redox Couple in Iron Phosphates. *Journal of the Electrochemical Society* **1997,** *144* (5), 1609-1613.

8. Coler, M. A.; Corren, S. A., Flexible Battery. US Patent 3023259A: 1962.

9. Bly, H. H., Flexible Battery. US Patent 2798896A: 1957.

10. Kutbee, A. T.; Bahabry, R. R.; Alamoudi, K. O.; Ghoneim, M. T.; Cordero, M. D.; Almuslem, A. S.; Gumus, A.; Diallo, E. M.; Nassar, J. M.; Hussain, A. M., Flexible and Biocompatible High-performance Solid-state Micro-battery for Implantable Orthodontic System. *npj Flexible Electronics* **2017,** *1* (1), 7.

11. Siegel, A. C.; Phillips, S. T.; Dickey, M. D.; Lu, N.; Suo, Z.; Whitesides, G. M., Foldable Printed Circuit Boards on Paper Substrates. *Advanced Functional Materials* **2010,** *20* (1), 28-35.

12. Hahn, R.; Reichl, H. In *Batteries and Power Supplies for Wearable and Ubiquitous Computing*, Third International Symposium on Wearable Computers, IEEE: 1999; p 168.

13. Coleman, J. P.; Lynch, A. T.; Madhukar, P.; Wagenknecht, J. H., Printed, Flexible Electrochromic Displays Using Interdigitated Electrodes. *Solar Energy Materials and Solar Cells* **1999,** *56* (3-4), 395-418.

14. Wang, Z.; Meng, X.; Chen, K.; Mitra, S., Synthesis of Carbon Nanotube Incorporated Metal Oxides for the Fabrication of Printable, Flexible Nickel-zinc Batteries. *Advanced Materials Interfaces* **2018,** *5* (4), 1701036.

15. Wang, B.; Ryu, J.; Choi, S.; Song, G.; Hong, D.; Hwang, C.; Chen, X.; Wang, B.; Li, W.; Song, H. K., Folding Graphene Film Yields High Areal Energy Storage in Lithium-Ion Batteries. *ACS Nano* **2018,** *12* (2), 1739-1746.

16. Wang, Z.; Meng, X.; Wu, Z.; Mitra, S., Development of Flexible Zinc-Air Battery with Nanocomposite Electrodes and a Novel Separator. *Journal of Energy Chemistry* **2017,** *26* (1), 129-138.

17. Gao, Z.; Song, N.; Zhang, Y.; Li, X., Cotton-textile-enabled, Flexible Lithium-ion Batteries with Enhanced Capacity and Extended Lifespan. *Nano Letters* **2015,** *15* (12), 8194-8203.

18. Wang, Z.; Wu, Z.; Bramnik, N.; Mitra, S., Fabrication of High-performance Flexible Alkaline Batteries by Implementing Multiwalled Carbon Nanotubes and Copolymer Separator. *Advanced Materials* **2014,** *26* (6), 970-976.

19. Liu, J.; Chen, M.; Zhang, L.; Jiang, J.; Yan, J.; Huang, Y.; Lin, J.; Fan, H. J.; Shen, Z. X., A Flexible Alkaline Rechargeable Ni/Fe Battery Based on Graphene Foam/Carbon Nanotubes Hybrid Film. *Nano Letters* **2014,** *14* (12), 7180-7187.

20. Yu, X.; Fu, Y.; Cai, X.; Kafafy, H.; Wu, H.; Peng, M.; Hou, S.; Lv, Z.; Ye, S.; Zou, D., Flexible Fiber-type Zinc-Carbon Battery Based on Carbon Fiber Electrodes. *Nano Energy* **2013,** *2* (6), 1242-1248.

21. Noerochim, L.; Wang, J.Z.; Chou, S.L.; Wexler, D.; Liu, H.K., Free-standing Single-walled Carbon Nanotube/SnO_2 Anode Paper for Flexible Lithium-ion Batteries. *Carbon* **2012,** *50* (3), 1289-1297.

22. Chandra, D.; Chien, W. M.; Talekar, A., Metal Hydrides for NiMH Battery Applications. *Mater. Matters* **2011,** *6*, 48-53.

23. Tarascon, J.-M.; Armand, M., Issues and Challenges Facing Rechargeable Lithium Batteries. *Nature* **2001,** *414* (6861), 359-367.

24. Etacheri, V.; Marom, R.; Elazari, R.; Salitra, G.; Aurbach, D., Challenges in the Development of Advanced Li-ion Batteries: A Review. *Energy & Environmental Science* **2011,** *4* (9), 3243-3262.

25. Singh, D., Characteristics and Effects of γ-NiOOH on Cell Performance and a Method to Quantify It in Nickel Electrodes. *Journal of the Electrochemical Society* **1998,** *145* (1), 116-120.

26. Papp, J. K.; Forster, J. D.; Burke, C. M.; Kim, H. W.; Luntz, A. C.; Shelby, R. M.; Urban, J. J.; McCloskey, B. D., Poly (Vinylidene Fluoride)(PVDF) Binder Degradation in Li-O_2 Batteries: A Consideration for the Characterization of Lithium Superoxide. *The Journal of Physical Chemistry Letters* **2017,** *8* (6), 1169-1174.

27. Matsuda, Y.; Morita, M.; Hanada, T.; Kawaguchi, M., A New Negative Electrode Matrix, BC_2N, for Rechargeable Lithium Batteries. *Journal of Power Sources* **1993,** *43* (1-3), 75-80.

28. Kannan, A.; Shukla, A.; Sathyanarayana, S., Oxide-Based Bifunctional Oxygen Electrode for Rechargeable Metal/Air Batteries. *Journal of Power Sources* **1989,** *25* (2), 141-150.

29. Rathika, R.; Padmaraj, O.; Suthanthiraraj, S. A., Electrical Conductivity and Dielectric Relaxation Behaviour of PEO/PVDF-Based Solid Polymer Blend Electrolytes for Zinc Battery Applications. *Ionics* **2018,** *24* (1), 243-255.

30. Wu, G.; Lin, S.; Yang, C., Preparation and Characterization of PVA/PAA Membranes for Solid Polymer Electrolytes. *Journal of Membrane Science* **2006,** *275* (1-2), 127-133.

31. Leonard, J. F.; Vukson, S.; Fritts, D. H.; Kim, K. Y., Electrical Battery Cell Wicking Structure and Method. US Patent USH858H: 1990.

32. Wang, T.; Hu, P.; Zhang, C.; Du, H.; Zhang, Z.; Wang, X.; Chen, S.; Xiong, J.; Cui, G., Nickel Disulfide-graphene Nanosheets Composites with Improved Electrochemical Performance for Sodium Ion Battery. *ACS Applied Materials & Interfaces* **2016,** *8* (12), 7811-7817.

33. Wang, Z.; Bramnik, N.; Roy, S.; Di Benedetto, G.; Zunino, J. L.; Mitra, S., Flexible Zinc-Carbon Batteries with Multiwalled Carbon Nanotube/conductive Polymer Cathode Matrix. *Journal of Power Sources* **2013,** *237*, 210-214.

34. Lin, M. C.; Gong, M.; Lu, B.; Wu, Y.; Wang, D.-Y.; Guan, M.; Angell, M.; Chen, C.; Yang, J.; Hwang, B. J., An Ultrafast Rechargeable Aluminium-ion Battery. *Nature* **2015,** *520* (7547), 324.

35. Wang, H.; Liang, Y.; Gong, M.; Li, Y.; Chang, W.; Mefford, T.; Zhou, J.; Wang, J.; Regier, T.; Wei, F., An Ultrafast Nickel–Iron Battery from Strongly Coupled Inorganic Nanoparticle/Nanocarbon Hybrid Materials. *Nature Communications* **2012,** *3*, 917.

36. Xu, G.-L.; Li, Y.; Ma, T.; Ren, Y.; Wang, H. H.; Wang, L.; Wen, J.; Miller, D.; Amine, K.; Chen, Z., PEDOT-PSS Coated ZnO/C Hierarchical Porous Nanorods as Ultralong-life Anode Material for Lithium Ion Batteries. *Nano Energy* **2015,** *18*, 253-264.

37. Huang, Y. H.; Goodenough, J. B., High-Rate $LiFePo_4$ Lithium Rechargeable Battery Promoted by Electrochemically Active Polymers. *Chemistry of Materials* **2008,** *20* (23), 7237-7241.

38. Huot, J. Y.; Boubour, E., Electrochemical Performance of Gelled Zinc Alloy Powders in Alkaline Solutions. *Journal of Power Sources* **1997,** *65* (1-2), 81-85.

39. Guo, L.; Deng, J.; Wang, G.; Hao, Y.; Bi, K.; Wang, X.; Yang, Y., N, P-Doped CoS_2 Embedded in TiO_2 Nanoporous Films for Zn-Air Batteries. *Advanced Functional Materials* **2018**, 1804540.

40. Peng, X.; Zhang, X.; Wang, L.; Xu, M.; Zhao, D.; Rui, Y.; Xu, J.; Tang, K., Fabrication of Zn_2GeO_4 Nanorods@ TiO_2 as Anodes for Lithium-ion Batteries with Enhanced Cycling Stability. *Materials Letters* **2016,** *185*, 307-310.

41. Dobryszycki, J.; Biallozor, S., On Some Organic Inhibitors of Zinc Corrosion in Alkaline Media. *Corrosion Science* **2001,** *43* (7), 1309-1319.

42. Park, D. J.; Aremu, E. O.; Ryu, K. S., Bismuth Oxide as an Excellent Anode Additive for Inhibiting Dendrite Formation in Zinc-Air Secondary Batteries. *Applied Surface Science* **2018,** *456*, 507-514.

43. Jain, R.; Adler, T.; McLarnon, F.; Cairns, E., Development of Long-lived High-performance Zinc-Calcium/Nickel Oxide Cells. *Journal of Applied Electrochemistry* **1992,** *22* (11), 1039-1048.

44. Brunetti, F. G.; Herrero, M. A.; Munoz, J. d. M.; Díaz-Ortiz, A.; Alfonsi, J.; Meneghetti, M.; Prato, M.; Vázquez, E., Microwave-induced Multiple Functionalization of Carbon Nanotubes. *Journal of the American Chemical Society* **2008,** *130* (25), 8094-8100.

45. Wang, Y.; Iqbal, Z.; Mitra, S., Microwave-induced Rapid Chemical Functionalization of Single-walled Carbon Nanotubes. *Carbon* **2005,** *43* (5), 1015-1020.

46. MacKenzie, K.; Dunens, O.; Harris, A. T., A Review of Carbon Nanotube Purification by Microwave Assisted Acid Digestion. *Separation and Purification Technology* **2009,** *66* (2), 209-222.

47. Bernardes, A.; Espinosa, D. C. R.; Tenório, J. S., Recycling of Batteries: A Review of Current Processes and Technologies. *Journal of Power Sources* **2004,** *130* (1-2), 291-298.

48. Hahn, R.; Reichl, H. In *Batteries and Power Supplies for Wearable and Ubiquitous Computing*, Wearable Computers, 1999. Digest of Papers. The Third International Symposium on, 18-19 Oct. 1999; 1999; pp 168-169.

49. Mohammed, M. G.; Kramer, R., All-printed Flexible and Stretchable Electronics. *Advanced Materials* **2017**.

50. Cheng, X.; Zhou, L.; Lu, Y.; Xu, W.; Zhang, P.; Lu, X., Facile Activation of Commercial Ni Foil as Robust Cathode for Advanced Rechargeable Ni-Zn Battery. *Electrochimica Acta* **2018,** *263*, 311-317.

51. Zeng, Y.; Meng, Y.; Lai, Z.; Zhang, X.; Yu, M.; Fang, P.; Wu, M.; Tong, Y.; Lu, X., An Ultrastable and High-Performance Flexible Fiber-Shaped Ni–Zn Battery Based on a Ni–NiO Heterostructured Nanosheet Cathode. *Advanced Materials* **2017,** *29* (44), 1702698.

52. Lau, X. C.; Wu, Z.; Mitra, S., Enhanced Charge-Carrier Transport through Shorter Carbon Nanotubes in Organic Photovoltaics. *ACS applied materials & interfaces* **2014,** *6* (3), 1640-1645.

53. Lau, X. C.; Wang, Z.; Mitra, S., A C70-carbon Nanotube Complex for Bulk Heterojunction Photovoltaic Cells. *Applied Physics Letters* **2013,** *103* (24), 243108.

54. Cheng, Y.-b.; Pascoe, A.; Huang, F.; Peng, Y., Print Flexible Solar Cells. *Nature* **2016,** *539* (7630), 488-489.

55. Ma, M.; Tang, Q.; Yang, P.; He, B., Room-Temperature Fabrication of Multi-Deformable Perovskite Solar Cells Made in a Three-Dimensional Gel Framework. *RSC Advances* **2016,** *6* (86), 82933-82940.

56. Gao, Z.; Yang, W.; Yan, Y.; Wang, J.; Ma, J.; Zhang, X.; Xing, B.; Liu, L., Synthesis and Exfoliation of Layered α-$Co(OH)_2$ Nanosheets and Their Electrochemical Performance for Supercapacitors. *European Journal of Inorganic Chemistry* **2013,** *2013* (27), 4832-4838.

57. Hiralal, P.; Imaizumi, S.; Unalan, H. E.; Matsumoto, H.; Minagawa, M.; Rouvala, M.; Tanioka, A.; Amaratunga, G. A. J., Nanomaterial-Enhanced All-Solid Flexible Zinc−Carbon Batteries. *ACS Nano* **2010,** *4* (5), 2730-2734.

58. Gaikwad, A. M.; Whiting, G. L.; Steingart, D. A.; Arias, A. C., Highly Flexible, Printed Alkaline Batteries Based on Mesh-embedded Electrodes. *Advanced Materials* **2011,** *23* (29), 3251-3255.

59. Park, J.; Park, M.; Nam, G.; Lee, J.S.; Cho, J., All-solid-state Cable-type Flexible Zinc–Air Battery. *Advanced Materials* **2015,** *27* (8), 1396-1401.

60. Gaikwad, A. M.; Khau, B. V.; Davies, G.; Hertzberg, B.; Steingart, D. A.; Arias, A. C., A High Areal Capacity Flexible Lithium-ion Battery with a Strain-compliant Design. *Advanced Energy Materials* **2015,** *5* (3), 1401389-n/a.

61. Ihlefeld, J. F.; Clem, P. G.; Doyle, B. L.; Kotula, P. G.; Fenton, K. R.; Apblett, C. A., Fast Lithium-ion Conducting Thin-film Electrolytes Integrated Directly on Flexible Substrates for High-power Solid-state Batteries. *Advanced Materials* **2011,** *23* (47), 5663-5667.

62. Ghaemi, M.; Amrollahi, R.; Ataherian, F.; Kassaee, M. Z., New Advances on Bipolar Rechargeable Alkaline Manganese Dioxide–zinc Batteries. *Journal of Power Sources* **2003,** *117* (1-2), 233-241.

63. Shen, Y.; Kordesch, K., The Mechanism of Capacity Fade of Rechargeable Alkaline Manganese Dioxide Zinc Cells. *Journal of power sources* **2000,** *87* (1-2), 162-166.

64. Stani, A.; Taucher-Mautner, W.; Kordesch, K.; Daniel-Ivad, J., Development of Flat Plate Rechargeable Alkaline Manganese Dioxide-Zinc Cells. *Journal of Power Sources* **2006,** *153* (2), 405-412.

65. Wang, Z.; Mitra, S., Development of Flexible Secondary Alkaline Battery with Carbon Nanotube Enhanced Electrodes. *Journal of Power Sources* **2014,** *266*, 296-303.

66. Payer, G.; Ebil, Ö., Zinc Electrode Morphology Evolution in High Energy Density Nickel-Zinc Batteries. *Journal of Nanomaterials* **2016,** *2016*, 39.

67. Phillips, J.; Mohanta, S., Electrolyte Composition for Nickel-Zinc Batteries. Google Patents: 2010.

68. Wang, Z.; Meng, X.; Chen, K.; Mitra, S., Synthesis of Carbon Nanotube Incorporated Metal Oxides for the Fabrication of Printable, Flexible Nickel-Zinc Batteries. *Advanced Materials Interfaces* **2018,** *5* (4), 1701036.

69. Zhang, H.; Wang, R.; Lin, D.; Zeng, Y.; Lu, X., Ni-based Nanostructures as High-performance Cathodes for Rechargeable Ni−Zn Battery. *ChemNanoMat* **2018,** *4* (6), 525-536.

70. Zeng, Y.; Lai, Z.; Han, Y.; Zhang, H.; Xie, S.; Lu, X., Oxygen-vacancy and Surface Modulation of Ultrathin Nickel Cobaltite Nanosheets as a High-energy Cathode for Advanced Zn-ion Batteries. *Advanced Materials* **2018,** *0* (0), 1802396.

71. Huang, Y.; Ip, W. S.; Lau, Y. Y.; Sun, J.; Zeng, J.; Yeung, N. S. S.; Ng, W. S.; Li, H.; Pei, Z.; Xue, Q.; Wang, Y.; Yu, J.; Hu, H.; Zhi, C., Weavable, Conductive Yarn-based NiCo/Zn Textile Battery with High Energy Density and Rate Capability. *ACS Nano* **2017,** *11* (9), 8953-8961.

72. Yuan, Y.; Xia, X.; Wu, J.; Yang, J.; Chen, Y.; Guo, S., Nickel Foam-supported Porous $Ni(OH)_2$/NiOOH Composite Film as Advanced Pseudocapacitor Material. *Electrochimica Acta* **2011,** *56* (6), 2627-2632.

73. Fu, X.Z.; Wang, X.; Xu, Q. C.; Li, J.; Xu, J.Q.; Lin, J.D.; Liao, D.W., Physical Characterization, Electrochemical Performance and Storage Stability of Spherical Al-substituted γ-NiOOH. *Electrochimica acta* **2007,** *52* (5), 2109-2115.

74. Ma, L.; Zhuang, H. L.; Wei, S.; Hendrickson, K. E.; Kim, M. S.; Cohn, G.; Hennig, R. G.; Archer, L. A., Enhanced Li-S Batteries Using Amine-functionalized Carbon Nanotubes in the Cathode. *ACS nano* **2015,** *10* (1), 1050-1059.

75. Wang, Z.; Wu, Z.; Di Benedetto, G.; Zunino, J. L.; Mitra, S., Microwave Synthesis of Highly Oxidized and Defective Carbon Nanotubes for Enhancing the Performance of Supercapacitors. *Carbon* **2015,** *91*, 103-113.

76. Zhao, Y.; Wu, W.; Li, J.; Xu, Z.; Guan, L., Encapsulating MWNTs into Hollow Porous Carbon Nanotubes: A Tube-in-tube Carbon Nanostructure for High performance Lithium-Sulfur Batteries. *Advanced Materials* **2014,** *26* (30), 5113-5118.

77. Wu, Z.; Wang, Z.; Yu, F.; Thakkar, M.; Mitra, S., Variation in Chemical, Colloidal and Electrochemical Properties of Carbon Nanotubes with the Degree of Carboxylation. *Journal of Nanoparticle Research* **2017,** *19* (1), 16.

78. Gong, M.; Li, Y.; Zhang, H.; Zhang, B.; Zhou, W.; Feng, J.; Wang, H.; Liang, Y.; Fan, Z.; Liu, J., Ultrafast High-capacity NiZn Battery with Nialco-layered Double Hydroxide. *Energy & Environmental Science* **2014,** *7* (6), 2025-2032.

79. Mohamad, A.; Haliman, H.; Sulaiman, M.; Yahya, M.; Ali, A., Conductivity Studies of Plasticized Anhydrous PEO-KOH Alkaline Solid Polymer Electrolyte. *Ionics* **2008,** *14* (1), 59-62.

80. Lewandowski, A.; Zajder, M.; Frąckowiak, E.; Beguin, F., Supercapacitor Based on Activated Carbon and Polyethylene Oxide-KOH-H_2O Polymer Electrolyte. *Electrochimica Acta* **2001,** *46* (18), 2777-2780.

81. Brandrup, J.; Immergut, E. H.; Grulke, E. A.; Abe, A.; Bloch, D. R., *Polymer Handbook*. Wiley New York etc: 1989; Vol. 7.

82. Biswas, S.; Vijayan, K., Friction and Wear of PTFE—a Review. *Wear* **1992,** *158* (1-2), 193-211.

83. Dunitz, J. D.; Taylor, R., Organic Fluorine Hardly Ever Accepts Hydrogen Bonds. *Chemistry–A European Journal* **1997,** *3* (1), 89-98.

84. Zhang, S. S.; Foster, D.; Read, J., Discharge Characteristic of a Non-aqueous Electrolyte Li/O_2 Battery. *Journal of Power Sources* **2010,** *195* (4), 1235-1240.

85. Ng, L. S.; Mohamad, A. A., Protonic Battery Based on a Plasticized Chitosan-Nh4no3 Solid Polymer Electrolyte. *Journal of Power Sources* **2006,** *163* (1), 382-385.

86. Amaral, M. M.; Raele, M. P.; Caly, J. P.; Samad, R. E.; Vieira, N. D.; Freitas, A. Z. In *Roughness Measurement Methodology According to Din 4768 Using Optical Coherence Tomography (Oct)*, SPIE Europe Optical Metrology, SPIE: 2009; p 8.

87. Ma, L.; Chen, S.; Li, H.; Ruan, Z.; Tang, Z.; Liu, Z.; Wang, Z.; Huang, Y.; Pei, Z.; Zapien, J. A.; Zhi, C., Initiating a Mild Aqueous Electrolyte Co_3O_4/Zn Battery with 2.2 V High Voltage and 5000-cycle Lifespan by a Co(III) Rich-Electrode. *Energy & Environmental Science* **2018**.

88. Yuan, Z.Z.; Zhou, Z. T.; Li, W. S., Cyclic Voltammetric Performance of Bi_2O_3 Particles on Abrasive Microelectrode. *Chinese Journal of Applied Cchemistry* **2004,** *21* (3), 255-259.

89. Hassan, M.; Arof, A., Ionic Conductivity in PEO-KOH Polymer Electrolytes and Electrochemical Cell Performance. *physica status solidi (a)* **2005,** *202* (13), 2494-2500.

90. Ma, L.; Chen, S.; Pei, Z.; Li, H.; Wang, Z.; Liu, Z.; Tang, Z.; Zapien, J. A.; Zhi, C., Flexible Waterproof Rechargeable Hybrid Zinc Batteries Initiated by Multifunctional Oxygen Vacancies-rich Cobalt Oxide. *ACS Nano* **2018**.

91. Vassal, N.; Salmon, E.; Fauvarque, J. F., Nickel/Metal Hydride Secondary Batteries Using an Alkaline Solid Polymer Electrolyte. *Journal of The Electrochemical Society* **1999,** *146* (1), 20-26.

92. Reddy, T. B., *Linden's Handbook of Batteries*. 4th Edition ed.; McGraw Hill Education (Asia) and Chemical Industry Press: China, 2013; p 540.

93. Manohar, A. K.; Malkhandi, S.; Yang, B.; Yang, C.; Prakash, G. S.; Narayanan, S., A High-performance Rechargeable Iron Electrode for Large-Scale Battery-based Energy Storage. *Journal of The Electrochemical Society* **2012,** *159* (8), A1209-A1214.

94. Chakkaravarthy, C.; Periasamy, P.; Jegannathan, S.; Vasu, K., The Nickel/Iron Battery. *Journal of Power Sources* **1991,** *35* (1), 21-35.

95. Halpert, G., Past Developments and the Future of Nickel Electrode Cell Technology. *Journal of Power Sources* **1984,** *12*, 177-192.

96. Chopard, B.; Herrmann, H.; Vicsek, T., Structure and Growth Mechanism of Mineral Dendrites. *Nature* **1991,** *353* (6343), 409.

97. Gaikwad, A. M.; Zamarayeva, A. M.; Rousseau, J.; Chu, H.; Derin, I.; Steingart, D. A., Highly Stretchable Alkaline Batteries Based on an Embedded Conductive Fabric. *Advanced Materials* **2012,** *24* (37), 5071-5076.

98. Tan, P.; Chen, B.; Xu, H.; Zhang, H.; Cai, W.; Ni, M.; Liu, M.; Shao, Z., Flexible Zn and Li-Air Batteries: Recent Advances, Challenges, and Future Perspectives. *Energy & Environmental Science* **2017,** *10* (10), 2056-2080.

99. Guan, C.; Zhao, W.; Hu, Y.; Ke, Q.; Li, X.; Zhang, H.; Wang, J., High-performance Flexible Solid-state Ni/Fe Battery Consisting of Metal Oxides Coated Carbon Cloth/Carbon Nanofiber Electrodes. *Advanced Energy Materials* **2016,** *6* (20), 1601034.

100. Liu, J.; Guan, C.; Zhou, C.; Fan, Z.; Ke, Q.; Zhang, G.; Liu, C.; Wang, J., A Flexible Quasi-solid-state Nickel-zinc Battery with High Energy and Power Densities Based on 3d Electrode Design. *Advanced Materials* **2016,** *28* (39), 8732-8739.

101. Saunier, J.; Alloin, F.; Sanchez, J.Y.; Caillon, G., Thin and Flexible Lithium-ion Batteries: Investigation of Polymer Electrolytes. *Journal of Power Sources* **2003,** *119*, 454-459.

102. Li, N. W.; Shi, Y.; Yin, Y. X.; Zeng, X. X.; Li, J. Y.; Li, C. J.; Wan, L. J.; Wen, R.; Guo, Y. G., A Flexible Solid Electrolyte Interphase Layer for Long-life Lithium Metal Anodes. *Angewandte Chemie International Edition* **2018,** *57* (6), 1505-1509.

103. Meng, X.; Wang, Z.; Di Benedetto, G.; Zunino III, J. L.; Mitra, S., Reducing Concentration Polarization and Enhancing the Performance of Flexible Nickel-Zinc Battery Using Polytetrafluoroethylene as Electrode Additive. *ChemistrySelect* **2018,** *3* (42), 11890-11894.

104. Gu, Y.; Federici, J., Fabrication of a Flexible Current Collector for Lithium Ion Batteries by Inkjet Printing. *Batteries* **2018,** *4* (3), 42.

105. Gaikwad, A.; Steingart, D., Printed Flexible Battery. US Patent App. 15/833,139: 2018.

106. Zhu, H.W.; Ge, J.; Peng, Y.C.; Zhao, H. Y.; Shi, L.A.; Yu, S. H., Dip-coating Processed Sponge-based Electrodes for Stretchable Zn-MnO_2 Batteries. *Nano Research* **2018,** *11* (3), 1554-1562.

107. Gong, Y.; Fu, K.; Xu, S.; Dai, J.; Hamann, T. R.; Zhang, L.; Hitz, G. T.; Fu, Z.; Ma, Z.; McOwen, D. W., Lithium-ion Conductive Ceramic Textile: A New Architecture for Flexible Solid-State Lithium Metal Batteries. *Materials Today* **2018**.

108. Wang, L.; Feng, X.; Ren, L.; Piao, Q.; Zhong, J.; Wang, Y.; Li, H.; Chen, Y.; Wang, B., Flexible Solid-state Supercapacitor Based on a Metal–organic Framework Interwoven by Electrochemically-deposited Pani. *Journal of the American Chemical Society* **2015,** *137* (15), 4920-4923.

109. Gao, H.; Hou, F.; Zheng, X.; Liu, J.; Guo, A.; Yang, D.; Gong, Y., Electrochemical Property Studies of Carbon Nanotube Films Fabricated by Cvd Method as Anode Materials for Lithium-ion Battery Applications. *Vacuum* **2015,** *112*, 1-4.

110. Pu, X.; Li, L.; Song, H.; Du, C.; Zhao, Z.; Jiang, C.; Cao, G.; Hu, W.; Wang, Z. L., A Self-charging Power Unit by Integration of a Textile Triboelectric Nanogenerator and a Flexible Lithium-ion Battery for Wearable Electronics. *Advanced Materials* **2015,** *27* (15), 2472-2478.

111. Gao, Z.; Song, N.; Li, X., Microstructural Design of Hybrid CoO@ NiO and Graphene Nano-Architectures for Flexible High Performance Supercapacitors. *Journal of Materials Chemistry A* **2015,** *3* (28), 14833-14844.

112. Zhi, M.; Xiang, C.; Li, J.; Li, M.; Wu, N., Nanostructured Carbon–Metal Oxide Composite Electrodes for Supercapacitors: A Review. *Nanoscale* **2013,** *5* (1), 72-88.

113. Chen, P.; Chen, H.; Qiu, J.; Zhou, C., Inkjet Printing of Single-walled Carbon Nanotube/RuO_2 Nanowire Supercapacitors on Cloth Fabrics and Flexible Substrates. *Nano Research* **2010,** *3* (8), 594-603.

114. Bao, L.; Zang, J.; Li, X., Flexible Zn_2SnO_4/MnO_2 Core/Shell Nanocable−Carbon Microfiber Hybrid Composites for High-performance Supercapacitor Electrodes. *Nano Letters* **2011,** *11* (3), 1215-1220.

115. Lau, X. C.; Wang, Z.; Mitra, S., Effect of Low Concentrations of Carbon Black in Organic Solar Cells. *Solar Energy Materials and Solar Cells* **2014,** *128*, 69-76.

116. Zhang, Y.; Gao, Z.; Song, N.; Li, X., High-Performance Supercapacitors and Batteries Derived from Activated Banana-Peel with Porous Structures. *Electrochimica Acta* **2016,** *222*, 1257-1266.

117. Biswal, M.; Banerjee, A.; Deo, M.; Ogale, S., From Dead Leaves to High Energy Density Supercapacitors. *Energy & Environmental Science* **2013,** *6* (4), 1249-1259.

118. Zang, J.; Li, X., In Situ Synthesis of Ultrafine β-MnO_2/polypyrrole Nanorod Composites for High-performance Supercapacitors. *Journal of Materials Chemistry* **2011,** *21* (29), 10965-10969.

119. Delahaye-Vidal, A.; Beaudoin, B.; Sac-Epée, N.; Tekaia-Elhsissen, K.; Audemer, A.; Figlarz, M., Structural and Textural Investigations of the Nickel Hydroxide Electrode. *Solid State Ionics* **1996,** *84* (3-4), 239-248.

120. Xu, Y.; Liu, Z.; Chen, D.; Song, Y.; Wang, R., Synthesis and Electrochemical Properties of Porous α-$Co(OH)_2$ and Co_3O_4 Microspheres. *Progress in Natural Science: Materials International* **2017,** *27* (2), 197-202.

121. Gao, X.P.; Yao, S.M.; Yan, T.Y.; Zhou, Z., Alkaline Rechargeable Ni/Co Batteries: Cobalt Hydroxides as Negative Electrode Materials. *Energy & Environmental Science* **2009,** *2* (5), 502-505.

122. Casellato, U.; Comisso, N.; Mengoli, G., Effect of Li Ions on Reduction of Fe Oxides in Aqueous Alkaline Medium. *Electrochimica Acta* **2006,** *51* (26), 5669-5681.

123. Reddy, T. B., *Linden's Handbook of Batteries*. 4th Edition ed.; McGraw Hill Professional: USA, 2010.

124. Binder, L.; Kordesch, K., Corrosion of Zinc Electrode Mixtures in Alkaline Media. *Journal of Electroanalytical Chemistry and Interfacial Electrochemistry* **1984,** *180* (1), 495-510.

125. Haupt, S.; Strehblow, H. H., Corrosion, Layer Formation, and Oxide Reduction of Passive Iron in Alkaline Solution: A Combined Electrochemical and Surface Analytical Study. *Langmuir* **1987,** *3* (6), 873-885.

126. Walsh, M. A., Rope Batteries. US Patent 4522897A: 1985.

127. Eshraghi, R. R., Fibrous Battery Cells. US Patent 6004691A: 1999.

128. Liljeback, P.; Stavdahl, O.; Beitnes, A. In *SnakeFighter-Development of a Water Hydraulic Fire Fighting Snake Robot*, 2006 9th International Conference on Control, Automation, Robotics and Vision, IEEE: 2006; pp 1-6.

129. Booth, J. W.; Shah, D.; Case, J. C.; White, E. L.; Yuen, M. C.; Cyr-Choiniere, O.; Kramer-Bottiglio, R., Omniskins: Robotic Skins That Turn Inanimate Objects into Multifunctional Robots. *Science Robotics* **2018,** *3* (22), 1853.